Abundance Estimates of False Killer Whales in Hawaiian Waters and the Broader Central Pacific

Amanda L. Bradford, Elizabeth A. Becker, Erin M. Oleson, Karin A. Forney, Jeff E. Moore, and Jay Barlow

Abundance Estimates of False Killer Whales in Hawaiian Waters and the Broader Central Pacific

Amanda L. Bradford[1], Elizabeth A. Becker[2,3], Erin M. Oleson[1],
Karin A. Forney[4], Jeff E. Moore[5], and Jay Barlow[5]

[1] Pacific Islands Fisheries Science Center, National Marine Fisheries Service
    1845 Wasp Boulevard
    Honolulu, HI 96818

[2] Institute of Marine Sciences, University of California Santa Cruz
    1156 High Street
    Santa Cruz, CA 95064

[3] Ocean Associates, Inc., under contract to Southwest Fisheries Science Center,
    National Marine Fisheries Service
    8901 La Jolla Shores Drive
    La Jolla, CA 92037

[4] Southwest Fisheries Science Center, National Marine Fisheries Service
    7544 Sandholt Road
    Moss Landing, CA 95039

[5] Southwest Fisheries Science Center, National Marine Fisheries Service
    8901 La Jolla Shores Drive
    La Jolla, CA 92037

U.S. Department of Commerce
Wilbur L. Ross, Jr., Secretary

National Oceanic and Atmospheric Administration
Neil A. Jacobs, Ph.D., Acting NOAA Administrator

National Marine Fisheries Service
Chris Oliver, Assistant Administrator for Fisheries

Table of Contents

List of Tables

List of Figures

Abstract

The abundance of two remote and broadly-distributed populations of false killer whales (*Pseudorca crassidens*) in Hawaiian waters was estimated using sighting data collected from ship-based, line-transect surveys conducted by NOAA Fisheries within the central Pacific between 1986−2017, including the three Hawaiian Islands Cetacean and Ecosystem Assessment Survey (HICEAS) efforts in the summer and fall of 2002, 2010, and 2017. The abundance of the Northwestern Hawaiian Islands (NWHI) population was estimated for 2010 and 2017 and of the pelagic population for each HICEAS year. Both design- and model-based line-transect analysis methods were used in the abundance estimation of the transboundary pelagic population, with the design-based approach estimating density uniformly within the U.S. Hawaiian Islands Exclusive Economic Zone (EEZ), and the model-based approach estimating density as a function of habitat covariates within the broader central Pacific and, from that, the EEZ. The design-based estimates of NWHI abundance in 2010 and 2017 are 878 (CV, 1.15; 95% CI, 145 to 5,329) and 477 (CV, 1.71; 95% CI, 48 to 4,712) individuals, respectively. The design-based estimates of pelagic false killer whale abundance in the EEZ in 2002, 2010, and 2017 are highly variable across years compared to the model-based estimates, although the average estimates over the three survey years are similar at 2,736 (CV, 0.53; 95% CI, 1,030 to 7,269) and 2,115 (CV, 0.34; 95% CI, 1,111 to 4,026) individuals for the design- and model-based approaches, respectively. Random variation in encounter rate and shifts in distribution within and around the EEZ are likely contributors to the variation in the design-based estimates. The combined use of these approaches strengthens the assessment and management of pelagic false killer whales by providing consistent abundance estimates for context-specific management applications. Ultimately, the model-based approach offers a more stable basis for managing pelagic false killer whales over time and allows for the estimation of abundance outside the EEZ, which is especially important for mitigating population-level impacts from longline fisheries.

Introduction

False killer whales (*Pseudorca crassidens*) are widely distributed in tropical and warm-temperate waters, but are considered rare throughout their range (Baird 2018). In the U.S. Exclusive Economic Zone surrounding the Hawaiian Islands (henceforth 'Hawaiian EEZ' for simplicity), genetic, photo-identification, and movement data have been used to differentiate three populations of false killer whales (Baird et al. 2008; Baird et al. 2010; Baird et al. 2013; Chivers et al. 2007; Chivers et al. 2010; Martien et al. 2014). Two of these populations are island-associated: one with the main Hawaiian Islands (MHI) (Baird et al. 2008; Baird et al. 2010; Baird et al. 2012), and the other with the Northwestern Hawaiian Islands (NWHI) (Baird et al. 2013). The MHI insular population is the best-studied false killer whale population worldwide (Baird et al. 2008; Baird et al. 2010; Baird et al. 2012; Baird et al. 2015; Bradford et al. 2018) and was listed as endangered under the U.S. Endangered Species Act in 2012[1], following a precipitous decline in abundance in the 1990s and current evidence of multiple threats to population recovery (Oleson et al. 2010). Less is known about the NWHI population, which was only relatively recently recognized as a unique population (Baird et al. 2013).

The third population is more broadly distributed in the pelagic waters of the Hawaiian EEZ and the broader central Pacific, although assessments of this transboundary population to date have been limited to the EEZ (Carretta et al. 2017). The pelagic population has a history of depredating bait and catch in the Hawaii-based pelagic longline fisheries (Bayless et al. 2017; Forney et al. 2011), which also extend from Hawaiian waters into the central Pacific. Bycatch associated with this depredation has previously exceeded allowable levels within the Hawaiian EEZ (Carretta et al. 2009), which led to the formation of a Take Reduction Team in 2010 and a Take Reduction Plan in 2012[2] to reduce serious injury and mortality of the population from fishing operations, as required by the U.S. Marine Mammal Protection Act (MMPA). Assessing the abundance and distribution of pelagic false killer whales throughout their range would improve ongoing efforts to measure and mitigate impacts from fisheries interactions.

Abundance estimates are important inputs in many conservation and management contexts and are a component of the Stock Assessment Reports mandated by the MMPA for marine mammal populations inhabiting U.S. waters, including transboundary populations. While the abundance of the MHI insular false killer whale population can be estimated using data from small-boat, photo-identification surveys around the MHI (Baird et al. 2008; Bradford et al. 2018), estimating the abundance of the less accessible NWHI and pelagic populations requires ship-based, line-transect surveys over a larger area (Bradford et al. 2014). NOAA Fisheries has carried out the Hawaiian Islands Cetacean and Ecosystem Assessment Survey (HICEAS) three times since the early 2000s to collect line-transect data necessary to estimate the abundance of cetaceans in the Hawaiian EEZ. The first HICEAS was conducted by the Southwest Fisheries Science Center (SWFSC) in 2002 and resulted in the first abundance estimates for most cetacean species in Hawaiian waters (Barlow 2006). False killer whales from the pelagic population were sighted during HICEAS 2002, leading to an abundance estimate of 484 (coefficient of variation or CV, 0.93; 95% confidence interval or CI, 103 to 2,274) individuals in the Hawaiian EEZ (Barlow and

---

[1] 77 Federal Register 70915 (28 November 2012)
[2] 77 Federal Register 71260 (29 November 2012)

Rankin 2007). HICEAS 2010 and HICEAS 2017 were carried out as a collaborative effort between the Pacific Islands Fisheries Science Center (PIFSC) and the SWFSC. False killer whales from the pelagic and NWHI populations were sighted during HICEAS 2010, leading to abundance estimates of 1,540 (CV, 0.67; 95% CI, 470 to 5,047) and 617 (CV, 1.11; 95% CI, 107 to 3,554) individuals, respectively, in the Hawaiian EEZ (Bradford et al. 2014; Bradford et al. 2015). Estimating false killer whale abundance from the HICEAS 2017 sighting data is a component of the present manuscript.

The previous false killer whale abundance estimates are based on standard design-based line-transect analysis methods (Buckland et al. 2001). Given the randomized survey design of each HICEAS, the estimates should be unbiased, a benefit of using a design-based approach (Thomas et al. 2007). However, design-based methods result in a single estimate of average density for the study area or survey strata, which can be limiting for management purposes that often require spatially-explicit estimates of density at finer scales (e.g., Redfern et al. 2017). In the case of pelagic false killer whales, these design-based estimates have additional limitations. Given their low occurrence, false killer whales are infrequently sighted, which results in small sample sizes that can be heavily influenced by random variation in the sampling process (Bradford et al. 2017). More importantly, the transboundary nature of the pelagic population, with the Hawaiian EEZ representing a jurisdictional and not a biological boundary, means that differences in the design-based estimates of abundance from 2002, 2010, and 2017 could represent real changes in abundance or simply shifts in distribution across the Hawaiian EEZ boundary. Distinguishing between these possibilities is important for management of mobile marine populations (Boyd et al. 2018; Forney 2000).

An alternative approach to analyzing line-transect data provides spatially-explicit density estimates in a study area based on a model of animal distribution (Hedley and Buckland 2004). These model-based line-transect methods estimate density as a function of habitat or spatial covariates and are a type of species distribution model (SDM; Guisan and Thuiller 2005). SDMs have become increasingly preferred for analyzing cetacean line-transect data (Bouchet et al. 2019) because they generally provide finer scale information on the density and distribution of cetaceans than design-based methods. Further, they do not require the same randomized survey design as design-based methods (Hedley and Buckland 2004) and can be extended temporally (e.g., Becker et al. 2014) and spatially (e.g., Mannocci et al. 2015) beyond the study period and area if care is taken not to extrapolate beyond the range of predictor values within the model. SDMs can generate more precise estimates than design-based methods, although they are more susceptible to bias if the model is not well-specified, so they are often paired with a design-based estimate as a point of comparison (Thomas et al. 2007). SDMs have been used to estimate the density of cetaceans in the Hawaiian EEZ and broader central Pacific, including for false killer whales (Becker et al. 2012; Forney et al. 2015). These models resulted in false killer whale abundance estimates in 2002 and 2010 that were similar to their corresponding design-based estimates, while demonstrating differences in distribution between those two survey years (Forney et al. 2015). However, the estimates were at relatively coarse spatial scales and were not population specific, such that their relevance to management was somewhat limited.

This study uses both design- and model-based line-transect approaches to estimate false killer whale density and abundance. The design-based approach is used to obtain density and abundance estimates of NWHI and pelagic false killer whales within the Hawaiian EEZ. The

2

model-based approach is used to evaluate pelagic false killer whale density and distribution in the broader central Pacific, provide density and abundance estimates for the Hawaiian EEZ, and examine temporal shifts in density and distribution relative to the Hawaiian EEZ. Both analysis approaches rely on pooled data from previous surveys in the central Pacific to estimate parameters. Thus, in addition to providing an abundance estimate for 2017, each method can be used to produce updated abundance estimates for 2002 and 2010 that maximize the use of all available data and account for changes in false killer whale data collection and analysis methods. A comparable set of abundance estimates of false killer whales in the Hawaiian EEZ and associated distributional inference from outside this boundary establishes a framework that can be used to evaluate the potential impacts of Hawaii-based and foreign longline fisheries on pelagic false killer whales.

Methods

Data Collection

Ship Surveys

Sighting rates of cetaceans in the Hawaiian EEZ are notably low (Barlow 2006; Bradford et al. 2017). As a result, sample sizes within a single HICEAS and even across all three HICEAS are too small to reliably estimate some parameters for the two density estimation approaches described here. Additionally, the SDM was developed specifically to evaluate pelagic false killer whale density and distribution in the broader central Pacific, such that sightings of false killer whales outside of the Hawaiian EEZ are important for building the associated habitat model. The SWFSC and PIFSC have been collecting cetacean line-transect data throughout the Pacific using consistent protocols (Kinzey et al. 2000) since 1986 and 2009, respectively. SWFSC and PIFSC line-transect surveys that focused on or transited through the central Pacific were compiled (Table 1) and sightings of false killer whales were extracted for use in the design- and model-based density estimation (Table 2; Appendix A).

Visual survey effort during all SWFSC and PIFSC surveys can be differentiated into two types: systematic and nonsystematic effort. Systematic effort occurred when the ship was on an established design-based transect line. However, the observers typically remained on-effort and followed standard observation protocols while transiting to and from ports, between transect lines, and during other survey-specific deviations from the transect lines. This latter type of survey effort is referred to as nonsystematic. Sightings of false killer whales made on systematic effort were used to estimate encounter rates and other parameters in both the design- and model-based line-transect density estimation (Table 2; Appendix A). Nonsystematic sightings were not suitable for estimating encounter rates in the design-based approach, but were used to estimate the detection function (the probability of detection as a function of perpendicular distance from the trackline) in the design-based approach and to develop encounter rate models for the SDM. Additionally, some nonsystematic and off-effort sightings were used to estimate the expected subgroup size for both approaches (see Density Estimation section below).

The visual observation teams consisted of six observers who rotated through three positions on the flying bridge of the ship and searched for cetaceans forward of the vessel, from 90° left to 90° right. The port and starboard observers searched using 25x binoculars, and the center data recorder used unaided eyes. When cetaceans were sighted, the initial bearing and radial distance to the sighting were recorded and used to compute the perpendicular distance from the trackline. When the sighting was within a strip width of 5.6 km (3 nmi) from the trackline, additional data collection steps took place so that species, species composition (for mixed-species groups), and group size could be determined (Kinzey et al. 2000).

HICEAS Effort

The design and implementation of the HICEAS in 2002, 2010, and 2017 have been described extensively (Barlow 2006; Bradford et al. 2014; Bradford et al. 2017; Yano et al. 2018). The following represents a brief summary of HICEAS-specific data collection as it relates to the present abundance analyses. Each HICEAS was conducted aboard two NOAA ships within the Hawaiian EEZ during the summer and fall. For HICEAS 2002, the study area was surveyed from the 52-m NOAA Ship *David Starr Jordan* (DSJ) from 6 August to 27 November 2002, and from

the 53-m NOAA Ship *McArthur* from 19 October to 25 November 2002 (Figure 1A). For HICEAS 2010, the study area was surveyed from the 68-m NOAA Ship *McArthur II* (MII) from 13 August to 1 December 2010, and from the 68-m NOAA Ship *Oscar Elton Sette* (OES) from 2 September to 29 October 2010 (Figure 1B). For HICEAS 2017, the study area was surveyed from the OES from 6 July to 10 October 2017, and from the 64-m NOAA Ship *Reuben Lasker* (LAS) from 26 August to 1 December 2017 (Figure 1C).

The survey design for each HICEAS consisted of parallel transect lines oriented WNW to ESE and spaced 85 km apart, providing comprehensive coverage of the study area (Barlow 2006; Bradford et al. 2014; Bradford et al. 2017; Yano et al. 2018). The HICEAS 2002 transect lines were used for HICEAS 2017, while the transect lines for HICEAS 2010 were placed midway between each of the HICEAS 2002 lines. HICEAS 2002 incorporated an MHI stratum with additional parallel transect lines added halfway between the main transect lines (Barlow 2006), resulting in a higher density of effort within 140 km of the MHI compared to the outer-EEZ stratum (Figure 1A). Systematic survey effort during HICEAS 2010 was unstratified (Bradford et al. 2014; Bradford et al. 2017) and thus was uniform throughout the Hawaiian EEZ (Figure 1B). During HICEAS 2017, systematic survey effort was again stratified between the MHI and the outer-EEZ, with the MHI stratum redefined to encompass the known ranges of several island-associated populations of cetaceans (Yano et al. 2018). The higher density of survey effort within the MHI stratum was accomplished not by additional parallel lines, but by surveying along routes used to deploy or recover drifting acoustic spar buoy recorders (DASBRs). DASBRs (not discussed further in this manuscript) were used to conduct finer-scale passive acoustic monitoring than could be achieved by the ship-based towed hydrophone array acoustic operations that were conducted simultaneously to but independently of the visual operations. The DASBR routes were originally assumed to represent randomized transects. However, an evaluation of the resulting effort found that it oversampled shallow areas closer to land and thus was not representative of the MHI stratum (Appendix B). Therefore, these fine-scale lines were treated as nonsystematic survey effort, and thus all systematic survey effort during HICEAS 2017 was uniform throughout the Hawaiian EEZ (Figure 1C).

False Killer Whales

Data collection for false killer whales has evolved as additional information about the behavior of this species has become available. Prior to HICEAS 2010, SWFSC and PIFSC line-transect data collection protocols for false killer whales were the same as those for most other cetaceans (Kinzey et al. 2000). That is, when visual observers sighted a false killer whale group while on-effort (systematic or nonsystematic), line-transect effort ceased, and the ship diverted from the trackline to allow the observers to verify species identification and to estimate group size. This type of survey effort, known as 'closing mode,' ensures more accurate species identity and group size estimates for the ensuing analysis, but can bias estimates of encounter rate compared to 'passing mode' effort when the ship remains on the trackline following a sighting (Schwarz et al. 2010). However, small-boat surveys around the MHI found that false killer whale groups comprise multiple subgroups spread out over many kilometers, requiring long encounters to count all individuals (Baird et al. 2008) and indicating that even the standard closing mode approach was likely leading to underestimates of false killer whale group size.

For this reason, a group-size estimation protocol was implemented during HICEAS 2010, which combined sightings and concurrent passive acoustic detections from the towed hydrophone array to locate and estimate the size of false killer whale subgroups (Bradford et al. 2014). Specifically, when false killer whales were sighted by the visual observers while on-effort, acoustic detections were used to direct the ship off the trackline to the perceived center of the group. When subgroups were detected, whether visually or acoustically, a subgroup size estimate was made by at least one observer. Passage through the group continued until no further subgroups were detected ahead of the beam of the ship by either method. The group-size estimation protocol was in keeping with the closing mode survey approach, but the extent of subgroup tracking and integration with acoustics was more extensive than a standard group close. In practice, the group-size estimation protocol was difficult to execute successfully, and the resulting data violated assumptions of line-transect sampling theory (Bradford et al. 2014). In particular, the HICEAS 2010 data revealed that false killer whale groups can span tens of kilometers, well beyond the transect strip width, and that subgroups, not groups, better represent a detectable unit for both line-transect data collection and analysis (Bradford et al. 2014). A subgroup-based analytical framework was thus used to analyze the HICEAS 2010 data, but careful retrospective treatment was required for the sightings collected using the group-size estimation protocol.

Following HICEAS 2010, a new two-phase, subgroup-based data collection protocol, referred to as the PC (for *Pseudorca crassidens*) protocol, was implemented during ship-based surveys conducted by the PIFSC. During phase 1 of the PC protocol, the ship remained in passing mode so that on-effort visual observers had the opportunity to detect subgroups within the trackline strip width and then obtain perpendicular distances from sighted subgroups to the trackline as needed for line-transect analysis. Phase 1 continued until there were no additional visual or acoustic detections ahead of the beam of the ship. In phase 2, the ship passed through the perceived center of the group to allow the observers to obtain size estimates for as many subgroups as possible. The PC protocol was standard operating procedure during HICEAS 2017.

Some additional details of the PC protocol are warranted (for the full protocol, see Appendix G of Yano et al. 2018). Phase 1 began when a false killer whale subgroup was detected within the established 5.6-km strip width while on-effort, regardless of whether the subgroup was detected visually or acoustically. However, if the subgroup was first detected acoustically, the visual observers were not alerted to the initiation of phase 1. False killer whale subgroups sighted forward of the vessel's beam by an on-effort visual observer during phase 1 were used in the density estimation. Subgroup sightings made past the beam of the ship or by an off-effort visual observer during phase 1 were considered to be off-effort sightings and were not used in the estimation. In contrast to phase 1, the visual observers were alerted to the initiation of phase 2. Subgroup sightings made in any direction from the ship by an on- or off-effort observer during phase 2 were logged as off-effort sightings, but the size estimates for these subgroups were used to compute the expected subgroup size parameter in the density estimation. Although phase 2 was developed to focus on subgroup size estimation, the visual observers were often able to estimate the size of sighted subgroups during phase 1. Subgroup size estimates made in either phase of the PC protocol consisted of an independent best, high, and low estimate from at least one visual observer.

Once group or subgroup size estimates were obtained and if weather conditions and animal behavior permitted, false killer whales were often approached by the ship or by a small boat launched from the ship for photo-identification and biopsy sampling to support individual and population identification. During HICEAS 2010 and HICEAS 2017, satellite tags were occasionally deployed from a small boat to track movements of individuals and to characterize the range of the three populations associated with the Hawaiian Islands. The photo-identification, genetic, and tagging data were used to assign each of the false killer groups sighted within the Hawaiian EEZ to one of the three populations based on established reference information (e.g., Baird et al. 2008; Baird et al. 2010; Baird et al. 2013; Chivers et al. 2007; Chivers et al. 2010; Martien et al. 2014). If population data were not collected and the sighting was made in an area of population overlap (Bradford et al. 2015), a prorated population assignment was made. These prorated assignments were based on the proportion of each population represented after compiling all PIFSC and SWFSC ship-based false killer whale sightings of known population in the area of population overlap.

Density Estimation

Line-transect Analysis

Line-transect analysis is a form of distance sampling that estimates animal density from four parameters: the detection function, expected cluster (in this case, subgroup) size, encounter rate, and probability of detection on the trackline, although the specific form of the density estimator can vary (Buckland et al. 2001). A design-based analysis approach estimates these parameters empirically and produces a single density estimate for the study area or each survey stratum. A model-based analysis approach estimates the encounter rate (and potentially expected cluster size) as a function of habitat covariates and corrects these model-based estimates for detectability. Density can thus be predicted at all locations within the study area where these habitat covariates can be measured, resulting in spatially-explicit estimates of density. In the present study, the parameters for the design- and model-based approaches were computed from the same data to the extent possible, although some differences were necessary to accommodate nuances of each framework. Below, the design-based methodology is presented first and includes a description of how each line-transect parameter was estimated. A summary of the model-based methodology follows and indicates how each parameter was adapted.

Design-based Approach

Analytical Framework

As described by Bradford et al. (2014), the conventional form of the line-transect estimator (i.e., the detection function does not include additional covariates) is the most appropriate for estimating the design-based density of false killer whales in the Hawaiian EEZ. The conventional form allows each parameter to be estimated separately using sightings from previous surveys to achieve sufficient sample sizes, with the exception of the encounter rate, which was computed using data only from the focal survey.

Specifically, for each HICEAS, the density, $D_{i,j}$, of false killer whales in population i (either the NWHI or pelagic) within the stock boundary of survey stratum j was estimated as follows:

$$D_{i,j} = \frac{n_{i,j} \cdot E(s) \cdot f(0)}{2 \cdot L_{i,j} \cdot g(0)_{i,j}} \qquad (1)$$

where $n_{i,j}$ is the number of systematic-effort subgroup sightings, $E(s)$ is the expected size (number of individuals) of false killer whale subgroups (assumed not to vary by population or stratum), $f(0)$ is the probability density function of the perpendicular detection distances evaluated at zero distance (also constant across population and stratum), $L_{i,j}$ is the length of systematic transect effort completed, and $g(0)_{i,j}$ is the probability of detecting an animal on the trackline (i.e., perpendicular distance = 0). The encounter rate (n_{ij}/L_{ij}) is the number of systematic-effort subgroup sightings divided by the length of transect lines surveyed on systematic effort and, like $g(0)_{i,j}$, is specific to population and stratum for each HICEAS. Bootstrap methods were used to obtain variances for all parameters. The design-based density estimation was implemented using custom code in the program R (R Core Team 2019) unless otherwise mentioned.

Detection Function
Sightings of false killer whales from the three HICEAS efforts were pooled with a subset of false killer whale sightings from other SWFSC and PIFSC line-transect surveys to achieve a sufficient sample size for modeling the detection function of subgroups (Bradford et al. 2014). Whereas Bradford et al. (2014) included sightings from the eastern tropical and central Pacific that were made in sighting conditions similar to those of the Hawaiian EEZ study area, the present analysis limited the pooled subset to sightings made from 5°S to 40°N, and from 175°E to 120°W, in the central Pacific to minimize potential heterogeneity between the geographical regions. The pooled sample included systematic and nonsystematic false killer whale sightings made between 1986 and 2017 (Appendix A). Like Bradford et al. (2014), for sightings made between 1986 and 2010, the initial sighting location was assumed to represent a single subgroup that may or may not have been a part of a larger group, making these sightings comparable to the initial subgroup detection of sightings made between 2011 to 2017. The 2011−2017 sightings were all made using the PC protocol. Therefore, all on-effort subgroup detections made during Phase 1 were included in the pool of sightings used to model the subgroup detection function.

False killer whales are rarely sighted with other species in the central Pacific, and there have been no mixed-species sightings of false killer whales in the Hawaiian EEZ since the implementation of the PC protocol. Since it is not possible to retrospectively account for the heterogeneity introduced by other species on the detection of false killer whale subgroups, only single-species sightings of false killer whales were used to model the subgroup detection function. However, the only systematic sighting of false killer whales during HICEAS 2002 was a mixed-species sighting, requiring careful consideration of whether this limitation on the detection function was appropriate. The details of the HICEAS 2002 sighting (DSJ-184; Table 2) documented by the observer who made the sighting revealed that subgroups of both false killer whales and bottlenose dolphins (*Tursiops truncatus*) were spread out over an area spanning approximately 5 km, but the species were described as behaving differently, with no indication that they were mixed at the subgroup level. Further, the observer did not specify what species was initially detected. Given these uncertainties, this sighting was excluded when fitting the detection function.

The 5−10% most distant subgroup detections in the pooled sample were truncated to improve model fit (Buckland et al. 2001), resulting in an analytical truncation distance of 4.5 km. A half-normal model (with no adjustments) was fitted to the perpendicular distance data because it exhibits greater stability when fitting cetacean sighting data (Gerrodette and Forcada 2005) and minimizes the effect of vessel attraction, which has been observed for false killer whales in the study area (Bradford et al. 2014). To address additional heterogeneity, an analysis was performed to evaluate the detection probabilities of the pooled subgroup detections as a function of perpendicular distance from the trackline and Beaufort sea state, a common factor affecting the detectability of cetaceans (Barlow et al. 2001). This analysis was considered to be exploratory given the lack of contrast in the covariate data. Specifically, only half of the Beaufort states (1, 3, and 4) were represented by more than 10 subgroup detections, and more than half of the detections were in Beaufort states 3 and 4. Including Beaufort sea state as a continuous covariate resulted in a lower AIC score than the model without the covariate, but the value was within two AIC units, and the $f(0)$ estimates only differed by 0.01, so the simpler model was used to estimate the detection function. The program Distance (Thomas et al. 2010) was used to estimate $f(0)$ and its inverse, the effective strip width (*ESW*), which is the distance from the trackline beyond which as many subgroups were detected as were missed within, and to obtain a bootstrap estimate (n = 5,000 iterations) of the CV.

Expected Subgroup Size
The implementation of the PC protocol during PIFSC line-transect surveys since 2011 has resulted in a sizable set of consistently collected subgroup size estimates made on-effort during the passing mode phase 1 and off-effort during the closing mode phase 2. At the time the PC protocol was developed, the expectation was that the observers would not regularly be able to produce confident estimates of subgroup size during phase 1, but this has not been the case. Further, it was anticipated that the phase 1 subgroup size estimates would be biased low, which has been shown for passing mode estimates of cetacean group size (Schwarz et al. 2010). To determine if the subgroup size estimates collected between 2011 and 2017 differed by phase, a generalized linear mixed model (GLMM) was used to evaluate the effect of PC protocol phase (treated as a factor variable) on subgroup size, which was calculated as the geometric mean of the "best" estimates (per Barlow 2006) made by each observer for each subgroup within the 4.5-km truncation distance. The GLMM used a gamma distribution and a log link, incorporated the sighting number as a random effect to account for the correlation between subgroup size estimates made during the same group, and was conducted using the R package 'lme4' (Bates et al. 2015). A lack of significant difference (small effect size with p-value $\geq$ 0.05) in subgroup size estimates between the two phases indicated that the subgroup sizes from both phases could be pooled to estimate $E(s)$. The subgroup sizes used to estimate $E(s)$ were randomly sampled with replacement 5,000 times to obtain an estimate of the CV for this parameter.

Trackline Detection Probability
The $g(0)$ estimate of 0.76 (CV, 0.14) for small groups of delphinids (Barlow 1995) was used in previous analyses of false killer whale abundance (e.g., Barlow 2006; Bradford et al. 2014; Forney et al. 2015). More recently, Barlow (2015) used pooled line-transect survey data from the eastern and central Pacific from 1986 to 2010 to derive $g(0)$ estimates specific to Beaufort state. The Beaufort-specific estimates indicated that $g(0)$ had previously been overestimated for most of the species evaluated, particularly for surveys with effort in high Beaufort states. False killer whales were not included in the Barlow (2015) analysis due to an insufficient number of

sightings in the pooled survey data. However, with the additional false killer whale sightings from PIFSC line-transect surveys from 2011−2017, sample sizes were sufficient to estimate Beaufort-specific $g(0)$ values for false killer whales using the methodology of Barlow (2015).

Systematic-effort sightings (including mixed-species sightings) within 5.5 km of the trackline during line-transect surveys conducted by SWFSC and PIFSC from 1986−2017 in the central and eastern tropical Pacific (Appendix A) were used to estimate relative $g(0)$ values for false killer whales. Mixed-species and eastern tropical Pacific sightings and a greater truncation distance than that of the detection function estimation were used to meet the sample size requirements of this method. The presence of a false killer whale sighting on a short transect segment (typically 10−15 km) was modeled as a binomial variable with the probability of occurrence given as a function of average Beaufort on that segment, year, and latitude and longitude, all treated as continuous variables following Barlow (2015). The model was fit within a generalized additive model (GAM; Hastie and Tibshirani 1990) framework using the R package 'mgcv' and a logit transformation (Wood 2017). The logarithm of the area effectively surveyed (the product of the segment length and Beaufort-specific estimates of *ESW*) was included in the model as an offset. *ESW* was modeled as a half-normal function with a multiple covariate model that included Beaufort as a continuous variable using the R package 'mrds' (Laake et al. 2018). Relative $g(0)$ values were assumed to be 1.0 in the best survey conditions (Beaufort sea states of 0 and 1 were pooled). Relative values in sea states 2 to 6 were inferred from the Beaufort effects in the model, assuming that the true density of false killer whales was not related to Beaufort state. Year and location (latitude and longitude) served as nuisance variables that helped control for spurious effects of varying sea states and false killer whale densities over time and space. CVs for the relative $g(0)$ values and estimates of *ESW* were estimated with a jackknife method (Barlow 2015).

In the absence of absolute estimates of $g(0)$ for false killer whales, the resulting relative values of $g(0)$ were treated as absolute values in the present density estimation. Estimates of $g(0)_{i,j}$ for each HICEAS were obtained by taking a weighted average of the Beaufort-specific values of $g(0)$, where the weights were the proportion of systematic effort in each Beaufort state (0−6) within the relevant stock boundary and survey stratum. The CV for each $g(0)_{i,j}$ estimate was obtained by a Monte Carlo approach, following methods used by Moore and Barlow (2017). The relative $g(0)$ values and associated CVs provided by the Barlow (2015) estimation approach are well approximated by the simple exponential function: $g(0)_b = \exp(\beta \cdot b)$, where b is the Beaufort state ($b = 0, 1,…, 6$) and $\beta = −0.36$ with a standard deviation (SD) of 0.11. A random normal variate β was drawn and the weighted average of $g(0)$ was calculated for each Monte Carlo sample (n = 10,000), and the CV of the $g(0)$ values was then computed across all samples. Bootstrap values (n = 5,000) of $g(0)_{i,j}$ were obtained by modeling it as a logit-transformed deviate with a mean and variance chosen to give the estimated $g(0)_{i,j}$ and CV.

Encounter Rate
With the implementation of the PC protocol, the encounter rate of NWHI and pelagic false killer whales during HICEAS 2017 was the sum of all phase 1 subgroups sighted during systematic effort within the truncation distance divided by the length of trackline surveyed within the stock boundary of each population in the Hawaiian EEZ. One systematic-effort sighting could not be assigned to a single population (OES-133; Table 2; Figure 1C) and therefore had a prorated population assignment. This prorated value was multiplied by the number of subgroups in the

associated sighting to estimate the expected number of detected subgroups in the relevant population.

The approach used to estimate the encounter rate of the NWHI and pelagic false killer whale populations during HICEAS 2010 replicated that detailed in Bradford et al. (2014). That is, the analysis was conducted as if phase 1 of the PC protocol had occurred, and the number of subgroups that would have been detected had the ship remained on the trackline was determined probabilistically. For the two systematic-effort sightings in which the group-size estimation protocol was successfully executed (MII-241 and OES-086; Table 2), perpendicular distances to sighted subgroups were calculated relative to a projected passing mode trackline (Figure C 1). Subgroups beyond the truncation distance were excluded from further consideration. The detection probability for the subgroup that represented the initial detection was assigned a value of 1 and for all others was calculated using the perpendicular distance of the subgroup from the trackline and the estimated detection function.

When the group-size estimation protocol was not successfully executed during HICEAS 2010 (i.e., the number, sizes, and locations of subgroups could not be determined) (MII-035; Table 2), an on-effort trackline was projected to the location of the initial detection (Figure C 1). The expected number of subgroups in the group was determined by dividing the estimate of total group size for the sighting by the point estimate of $E(s)$. The number of these subgroups within the truncation distance of the projected trackline was estimated by multiplying the expected number of subgroups in the group by the average proportion of subgroups within the truncation distance of the projected trackline for sightings MII-241 and OES-086. For the remaining subgroups, the first was assigned a detection probability of 100%, and all others were assigned the average detection probability for the study (i.e., ESW divided by the truncation distance). For the group-size estimation protocol sightings, the sum of the detection probabilities represented the expected number of subgroups that would have been detected had the ship remained in passing mode, and L_{ij} was adjusted to account for the length of the projected on-effort trackline.

While there was no concerted effort to account for subgroups during HICEAS 2002, the single false killer whale sighting made while on systematic effort (DSJ-184; Table 2) was also analyzed as if phase 1 of the PC protocol had occurred to ensure that the estimates of encounter rate were comparable across surveys. However, an on-effort trackline was not projected because the initial detection was made at 90 degrees from the ship (Figure C 2). All subgroups for this sighting were assumed to be within the truncation distance given the path of the ship when closing on the group, and subgroup-specific detection probabilities were estimated as for the HICEAS 2010 sighting MII-035. The sum of those probabilities represented the total number of expected subgroups that would have been detected if the vessel had remained in passing mode.

The number of detected subgroups (both actual and expected) across all sightings of a population within a survey stratum were summed to produce each n_{ij}. The variance of each encounter rate was estimated using a bootstrap procedure that sampled the trackline effort divided into 150-km segments, approximately the daily survey distance (Barlow 2006). Each bootstrap randomly sampled the effort segments and their associated false killer whale sightings with replacement 5,000 times. For bootstrap draws of sightings with an actual number of detected subgroups, the number of subgroups in that sighting contributed to the n_{ij} for that iteration of the bootstrap. For HICEAS 2017, when a segment was drawn with a sighting with a prorated population

assignment, the sighting was stochastically assigned to the relevant population with a probability equal to the prorated value. For HICEAS 2010, when a segment was drawn with a successful group-size estimation protocol sighting, the number of subgroups was stochastically determined based on the previously described estimated detection probabilities. For HICEAS 2010 and HICEAS 2002, when a segment was drawn with a sighting without localized subgroups, the number of subgroups was determined by drawing a random sample of subgroups from the observations used to estimate $E(s)$ until the sum of the subgroups equaled the total group size estimate associated with the sighting.

Abundance Estimation

For each HICEAS-specific survey stratum, the density (individuals per km^2) of false killer whales in either the pelagic or the NWHI population was calculated using Equation (1) with the point estimates of each parameter. Abundance was determined by multiplying the estimated density by the area of the survey stratum associated with each population (Figure 1). For pelagic false killer whales, this area was 2,447,635 km^2 for the Hawaiian EEZ (i.e., HICEAS 2010 and HICEAS 2017) and either 2,235,180 km^2 or 212,455 km^2 for the outer-EEZ or MHI stratum, respectively (i.e., HICEAS 2002). Note that as of this study, the inner stock boundary for the pelagic false killer whale population (Bradford et al. 2015) has been eliminated given the nearshore movements of two pelagic false killer whales tagged during HICEAS 2017 (Appendix D) . The area of the NWHI false killer whale stock boundary (449,801 km^2; Bradford et al. 2015) was used to calculate abundance for this population.

Variance in abundance (and density) was estimated by randomly combining the 5,000 bootstrap values of $f(0)$, $E(s)$, $n_{i,j}/L_{i,j}$, and $g(0)_{i,j}$ and calculating the CV and lognormal 95% CIs of the resulting bootstrap values of abundance. Total abundance for HICEAS 2002 was computed by summing the stratum-specific abundance point estimates. Overall density was then calculated by dividing the total abundance by the total area within the Hawaiian EEZ used by the population. The abundance estimates for each population were averaged over all HICEAS years to produce an average abundance estimate and associated CV (from summing the variances) and lognormal 95% CI during the study period.

Model-based Approach

Sighting Data

A subset of the compiled SWFSC and PIFSC surveys conducted in the central Pacific between 1997 and 2017 was identified as having suitable spatial and temporal overlap with available environmental data and therefore selected for use in the model-based estimation of pelagic false killer whale density (Table 1). All on-effort false killer whale sightings from the pelagic population (including prorated population assignments and mixed-species sightings) from this subset of surveys were used to build the SDM (Appendix A). Sightings made prior to 2011 were standardized to the PC protocol as previously described for the design-based approach in order to obtain the number of subgroups that would have been detected during phase 1 of the PC protocol. As none of these additional pre-2011 sightings involved localizing subgroups, this standardization involved the method used for sightings DSJ-184 and MII-035 (from HICEAS 2002 and HICEAS 2010, respectively), although like DSJ-184, it was not necessary to estimate the number of subgroups within the truncation distance because the ship remained within the truncation distance when closing on each group. The PC protocol was compromised during one

2013 sighting (i.e., OES-059; Appendix A) used to build the SDM. In this sighting, the ship closed on the group instead of staying in passing mode, although the subgroups were localized. Thus, this sighting was standardized to the PC protocol in the same way that sightings MII-241 and OES-086 from HICEAS 2010 were to estimate the subgroup encounter rate for the design-based approach.

The central Pacific study area of the SDM was defined to extend from the equator to 43°N, and from 175°E to 132°W, similar to Forney et al. (2015). Survey effort was concentrated in waters of the Hawaiian EEZ (Figure 2). Only on-effort data collected in Beaufort states 0−6 were used in model development. To create samples for modeling, continuous portions of on-effort survey tracklines were divided into approximate 10-km segments using methods described by Becker et al. (2010). False killer whale sighting data were truncated at 5.5 km perpendicular to the trackline to maximize sample size and maintain consistency with the Beaufort-specific *ESW* estimates produced as part of the relative $g(0)$ estimation, as Beaufort-specific values of both of these parameters were used in the SDM to estimate density. A detection function was not estimated as part of the SDM, so this approach was not subject to the same truncation constraints as the design-based approach (Buckland et al. 2001). All habitat covariates were derived based on the segment's geographical midpoint.

Environmental Covariate Data
Outputs from the Hybrid Coordinate Ocean Model (HYCOM[3]) were used as dynamic predictor variables of density in the SDM. HYCOM products include a global reanalysis that assimilates multiple sources of data in product development (including satellite and *in situ*), and outputs from HYCOM have been widely used and tested. Daily averages for each variable calculated at the 0.08 degree (~9km) horizontal resolution of the HYCOM output were used for model development. The suite of potential dynamic predictors included sea surface temperature (SST) and its standard deviation (sdSST), calculated for a 3×3-pixel box around the modeling segment midpoint, mixed layer depth (MLD, defined by a 0.5°C deviation from the SST), sea surface height (SSH), sdSSH, sea surface salinity (SAL), and sdSAL. Distance to land and water depth were also included as potential predictors, derived from the ETOPO1 1-arc-min global relief model (Amante and Eakins 2009) and obtained for the midpoint of each transect segment. The latitude and longitude of each segment midpoint were also offered as separate static covariates.

A tensor product smooth of latitude and each of the dynamic variables (Wood 2003) was included separately in the suite of potential predictors to account for latitudinal oceanic gradients within the central Pacific study area. Other modeling studies have successfully used such bivariate predictors to account for gradients in study areas that span a range of latitudes (Becker et al. 2016; Becker et al. 2018; Forney 2000; Palacios et al. 2019; Yuan et al. 2017). A tensor product smooth of latitude and longitude was not included to avoid extrapolating beyond the covariate range because parts of the study area were not surveyed (Figure 2).

Habitat-based Density Models
Predictions of pelagic false killer whale density were derived from encounter rate and group size models that were built using GAMs. Methods largely followed those described in Becker et al.

---

[3] Hybrid Coordinate Ocean Model, https://www.hycom.org

(2016), but were tailored to be as consistent as possible with data and parameters used for the design-based estimation. Group size models from previous false killer whale SDMs have used group size estimates from the observers without accounting for subgroup structure (e.g., Forney et al. 2015). Although the design-based estimates use subgroups as the detection unit, doing so within the SDM framework was challenged by the relatively small number of sightings and large variation in the number of subgroups per segment, creating significant overdispersion that could not be accurately modeled, even with the Tweedie distribution designed for overdispersed data (Miller et al. 2013). Therefore, groups were modeled using 'effective group sizes' (the total number of animals within all detected subgroups in a group) rather than subgroups and subgroup sizes. To derive an effective group size for each sighting, the number of subgroups detected (actual or expected, as determined in the design-based approach) was multiplied by the expected subgroup size ($E(s)$) used in the design-based analysis. Given the variation in effective group sizes (range = 1−26 individuals), separate encounter rate and group size models were developed. Encounter rate models were built using all transect segments, regardless of whether they included sightings, using the number of group-sightings per segment as the response variable and a Tweedie distribution to account for overdispersion. Effective-group size models were built using only those segments that included sightings, using the natural log of effective group size as the response variable and a Gaussian link function.

The full suite of potential habitat predictors was offered to both the encounter rate and group size GAMs, which were developed in R (R Core Team 2017) using the package 'mgcv' (Wood 2011). Although 'mgcv' is robust to correlated variables (Wood 2008), distance to land and depth (absolute correlation = 0.59) were offered to the models separately. The bivariate interaction terms between latitude and each of the dynamic variables (SST, SSH, SAL, and MLD) were also included individually to avoid overfitting and to aid in the ecological interpretation of the interaction term. In both models, restricted maximum likelihood (REML) was used to optimize the parameter estimates (Marra and Wood 2011). Potential variables were excluded from the model using a shrinkage approach that modifies the smoothing penalty, allowing the smooth to be identically zero and removed from the model (Marra and Wood 2011). Additionally, to avoid overfitting, variables that had p-values ≥ 0.05 were also removed; models were then refit to ensure that all remaining variables had p-values < 0.05 (Redfern et al. 2017; Roberts et al. 2016).

The encounter rate model included an offset, defined as the natural log of the effective area searched, A_k, on the 10-km effort segment k:

$$A_k = 2 \cdot L_k \cdot ESW_k \cdot g(0)_k \tag{2}$$

where L_k is the segment length, ESW_k is the effective strip width, and $g(0)_k$ is the probability of detection on the trackline. Following the methods of Becker et al. (2016), segment-specific estimates of both ESW and $g(0)$ were incorporated into the models based on the recorded Beaufort sea state conditions on that segment and the Beaufort-specific $g(0)$ and associated ESW estimates for false killer whales as described above for the design-based approach. Segment-specific predictions from the final encounter rate and group size models were combined to estimate false killer whale density, D_k, on segment k using the standard line-transect equation (Buckland et al. 2001):

14

$$D_k = \frac{m_k}{A_k} \cdot S_k \tag{3}$$

where m_k/A_k is model-derived encounter rate, and S_k is the model-derived effective group size.

Model performance was evaluated using established metrics, including the percentage of explained deviance, the area under the receiver operating characteristic curve (AUC; Fawcett 2006), the true skill statistic (TSS; Allouche et al. 2006), the ratio of observed (based on standard line-transect analyses of the 1997−2017 dataset that was used for modeling, without the inclusion of habitat variables) to predicted density (calculated for each segment and summed to obtain a study area density ratio), and visual inspection of predicted and observed distributions during the 1997–2017 cetacean surveys (Barlow et al. 2009; Becker et al. 2010; Becker et al. 2016; Forney et al. 2012). AUC discriminates between true-positive and false-positive rates, and values range from 0 to 1, where a score of > 0.5 indicates better than random discrimination. TSS accounts for both omission and commission errors and ranges from −1 to +1, where +1 indicates perfect agreement and values of zero or less indicate a performance no better than random. To calculate TSS, the sensitivity-specificity sum maximization approach (Liu et al. 2005) was used to obtain thresholds for species presence.

The encounter rate and group size habitat relationships derived from the complete 1997−2017 dataset were used to predict spatially-explicit density values for the full central Pacific study area, given the environmental conditions specific to the 2002, 2010, and 2017 HICEAS effort periods. Model predictions were made on separate tri-daily (3 sequential days) environmental conditions covering each of the three HICEAS effort periods. Daily predictions have been used for similar models developed for the California Current Ecosystem (Becker et al. 2018). However, given that the physical oceanographic properties of waters around the Hawaiian Archipelago are defined by larger-scale processes (Mann and Lazier 2005), a coarser temporal resolution was selected for the central Pacific study area. The tri-daily predictions were then averaged within each year to produce spatial grids of average 2002, 2010, and 2017 false killer whale density at 9-km^2 resolution within the study area. In addition, all of the predicted tri-daily false killer whale densities were averaged to provide a "multi-year average" estimate of false killer whale density in the central Pacific study area, taking into account the varying oceanographic conditions during HICEAS 2002, 2010, and 2017.

While the value of $E(s)$ used to estimate effective group size is robust to the difference in the design- and model-based truncation distances, it is possible that the number of detected subgroups in a group is biased in a limited number of cases because of the influence of the design-based truncation distance (e.g., expected numbers of subgroups determined using the average design-based detection probability). To examine potential bias in the model predictions due to uncertain estimation of effective group size (from both the use of design-based inputs as well as from changes in the group size data collection protocols between surveys), predictions from the encounter-rate model were evaluated separately to assess if the yearly (i.e., 2002, 2010, 2017) distribution patterns were driven solely by the group size model. The model predictions revealed similar patterns in distribution shifts with and without the addition of the group size model (Appendix E), so the spatially-explicit estimates of absolute abundance were based on the combination of predictions from the encounter rate and group size models.

Model-based abundance estimates were derived for both the larger central Pacific and nested Hawaiian EEZ study areas. The model-based abundance estimates were calculated as the sum of the individual grid cell abundance estimates, which were derived by multiplying the cell area (in km^2) by the predicted grid cell density, exclusive of any portions of the cells located outside the study areas or on land. Area calculations were completed using the R packages 'geosphere' and 'gpclib' (R Core Team 2017). Density and abundance for the Hawaiian EEZ were extracted from the overall central Pacific model by clipping the model predictions to the boundaries of the Hawaiian EEZ study area.

Uncertainty

Variation in environmental conditions has been shown to be one of the greatest sources of uncertainty within the model-based framework (Barlow et al. 2009; Forney et al. 2012). Spatially-explicit measures of uncertainty in density based on the environmental variability from 2002 to 2017 were calculated as pixel-specific standard errors based on the tri-daily predictions within each year or on the full set of tri-daily predictions for the multi-year average. In addition to the pixel-specific estimates of uncertainty, lognormal 95% CIs for the model-based abundance estimates were derived from the tri-daily variance estimates using standard formulae.

Uncertainty in detection parameters was quantified using the same general approach for obtaining each $g(0)_{i,j}$ CV in the design-based analysis but accounted for Beaufort dependence on both *ESW* and $g(0)$. Again, let $g(0)_b = \exp(\beta \cdot b)$, where b is the Beaufort state ($b = 0, 1,…, 6$) and $\beta = -0.36$ (SD = 0.11). Random values of β and the *ESW* function parameters were drawn from their empirical distributions for each of the Monte Carlo samples (n = 10,000). For each sample, a weighted estimate was obtained for the product $ESW \cdot g(0)$, where the weights were the proportions of effort in each Beaufort state. The CV of the weighted $ESW \cdot g(0)$ values was then computed across all samples.

The variance in effective group size was estimated using standard methods and also incorporated in the model-based estimates. These four sources of uncertainty (i.e., environmental variability, *ESW*, $g(0)$, and effective group size) were combined using the delta method (Seber 1982) to provide an overall measure of variance for the model-based abundance estimates. The derivation of spatially-explicit variance measures that account for these combined sources of uncertainty in an SDM is the subject of ongoing research[4] and beyond the scope of this analysis.

---

[4] U.S. Navy, Living Marine Resources Project 31. DenMod: Working Group for the Advancement of Marine Species Density Surface Modeling, https://www.navfac.navy.mil/content/dam/navfac/Specialty Centers/Engineering and Expeditionary Warfare Center/Environmental/lmr/LMRFactSheet_Project31.pdf

Results

Survey Sightings

Data from 79 false killer whale sightings (Appendix A) from 20 line-transect surveys (Table 1) of the central Pacific were used to derive the design-based and model-based parameter estimates within the present analysis. Although the majority of the sightings could be assigned to population using photo-identification, genetic, telemetry, or location information, nine sightings used in the design- or model-based encounter rate estimation could not be assigned to a population and required a prorated population assignment. The compiled ship-based false killer whale sightings of known population in the area where the NWHI and pelagic populations overlap (n = 5 sightings between 2010 and 2017) revealed an NWHI:pelagic proportion of 0.4:0.6. Similar treatment of sightings in the area of overlap between the MHI and pelagic populations (n = 10 sightings between 2005 and 2017) indicated an MHI:pelagic ratio of 0.8:0.2.

Design-based Estimates

Systematic visual effort for false killer whales in the Hawaiian EEZ encompassed a total of 17,013, 16,145, and 16,209 km of transects in Beaufort sea states from 0 to 6 during HICEAS 2002, 2010, and 2017, respectively, with 3,540 km of the total systematic effort in the MHI stratum in 2002 (Figure 1). The number of systematic-effort sightings of false killer whales made was 1, 6, and 9 during HICEAS 2002, 2010, and 2017, respectively (Table 2). Of the 16 systematic-effort false killer whale sightings made across all HICEAS effort, one was assigned to the MHI population (HICEAS 2017), one to the NWHI population (HICEAS 2010), 13 to the pelagic population (HICEAS 2002, 2010, and 2017), and one from HICEAS 2017 required a prorated assignment between the NWHI and pelagic populations (Table 2; Figure 1). Nine nonsystematic-effort sightings from HICEAS 2010 and 2017 were part of the pooled sample used to estimate the false killer whale detection function, and five nonsystematic-effort sightings and eight off-effort sightings from HICEAS 2017 contributed subgroup sizes for the estimation of $E(s)$ (Appendix A). An additional nine off-effort sightings were not used in the estimation because they could not contribute subgroup sizes to the $E(s)$ estimation: one from HICEAS 2002, five from HICEAS 2010, and three from HICEAS 2017.

A total of 54 false killer whale group sightings from the central Pacific were pooled to model the detection function (Appendix A). Incorporating 46 additional subgroup sightings from 2011 to 2017 that were made after the initial subgroup detection during Phase 1 of the PC protocol, the detection function was modeled using 100 subgroups in total. The pooled sample includes subgroup sightings that occurred disproportionately more often in the distance bin closest to the trackline (Figure 3). The resulting detection function (Figure 3) and bootstrap resampling produced an $f(0)$ estimate of 0.41 km^{-1} (CV, 0.10) (ESW = 2.43 km).

The 216 "best" estimates of subgroup size made by individual observers while on-effort during Phase 1 (n = 93) and while off-effort during Phase 2 (n = 123) of the PC protocol resulted in 127 subgroup size estimates (n = 63 phase 1, n = 64 phase 2) from 32 groups (Appendix A) once the geometric mean was taken of the "best" estimates for each subgroup (median of 1 observer estimate per subgroup, range 1−6) (Figure 4). The GLMM indicated that phase 2 subgroup sizes were not significantly different from those of phase 1 (predictor coefficient estimate = 0.04, Wald z = 0.32, p-value = 0.75). Given the lack of significant difference in subgroup size

estimates between the two phases, the subgroup size estimates were pooled and produced an $E(s)$ of 2.37 (CV, 0.06).

A total of 113 false killer whale sightings from the central (n = 51) and eastern tropical Pacific (n = 62) were pooled to estimate relative $g(0)$ values (Appendix A). Beaufort-specific estimates of trackline detection probability decreased monotonically from an assumed value of 1.00 in Beaufort states 0 and 1 to a value of 0.19 in Beaufort state 6 (Table 3). The proportions of systematic survey effort in each Beaufort state (0−6) within the relevant stock boundary and survey stratum used in the weighted average of the Beaufort-specific $g(0)$ values and associated CVs are shown in Appendix F, resulting in $g(0)_{i,j}$ estimates that range from 0.34 (CV, 0.33; HICEAS 2017 pelagic population) to 0.40 (CV, 0.29; HIICEAS 2010 NWHI population) (Table 4).

The sighting-specific contributions to the encounter rate produced n_{ij} values that are summarized along with L_{ij}, the number of 150-km effort segments for the bootstrap, n_{ij}/L_{ij}, and the bootstrap CV estimate in Table 4. Estimates of false killer whale density and abundance during HICEAS 2002, 2010, and 2017 were highly variable (Table 5). Estimates are available for the NWHI population in two years (2010 and 2017) and for the pelagic population in all three HICEAS years. Since no false killer whales were sighted in the MHI stratum during HICEAS 2002, only the EEZ-wide estimate of pelagic abundance is reported.

Model-based Estimates

The habitat-based density model for the pelagic stock of false killer whales was developed using 113,654 km of on-effort survey data collected during 14 surveys between 1997 and 2017 within the central Pacific study area in Beaufort sea state conditions 0−6 (Table 1; Figure 2). The majority (53%) of this effort was from the HICEAS surveys (59,768 km). Despite the inclusion of 10 years of survey data, only 38 sightings were available for modeling (Appendix A), with the majority of these within the Hawaiian EEZ (Figure 2). Nine of these sightings involved a prorated assignment to the pelagic population with four sightings within the overlap area of the NWHI and pelagic populations and five sightings in the overlap area of the MHI and pelagic populations (Appendix A).

Predictor variables included in the encounter rate model were SST, the standard deviation of SST, and the smooth of SSH and latitude, and the group size model included mixed layer depth, with a combined explained deviance of 17.5% (Appendix G). The greatest number of pelagic false killer whales was predicted to occur in warm waters with shallow mixed layer depth and high deviations in sea surface temperature (Figure 5). The bivariate SSH:latitude function suggests that higher densities of pelagic false killer whales are found in intermediate SSH values rather than in areas with low or high values, but that this effect decreases with increasing latitude (Figure 5). The ratio of observed to predicted density for the central Pacific study area was 1.00, indicating that the model-based density predictions were consistent with those derived from standard line-transect analyses. Similarity between the two separately-derived density estimates provides general confidence in model performance. Reasonable model performance was also indicated by an AUC value of 0.70 and a TSS value of 0.34.

Similar to previous habitat models developed for false killer whales in the central North Pacific (Becker et al. 2012; Forney et al. 2015), the map of multi-year average density shows the highest

predicted densities near the equator, particularly in the eastern tropical Pacific, with the lowest predicted densities in the northeastern portion of the study area (Figure 6A). Maps of the lower and upper 90% CI also demonstrate the prevalence of false killer whales near the equator and in the eastern tropical Pacific (Figure 6C−D). The 2002, 2010, and 2017 density maps reveal interannual shifts in distribution throughout the central Pacific, including variation in predicted density within the Hawaiian EEZ (Figure 7B−D). The multi-year average density map specific to the Hawaiian EEZ study area shows highest predicted densities within the lee of the MHI (Figure 8A), as does the upper-90% CI (Figure 8D). Rescaling the density predictions into linear increments specific to the Hawaiian EEZ study area indicates yearly changes in the distribution of false killer whales (Figure 9).

Model-predicted abundance estimates indicate that for the central Pacific study area, the greatest number of pelagic false killer whales were present in 2017, and the lowest in 2010 (Table 6). Conversely, the Hawaiian EEZ model-based abundance estimates were greatest in 2010 and lowest in 2017, although they were more similar among years than estimates for the broader central Pacific study area (Table 6). The spatially-explicit density maps for the central Pacific study area suggest distribution shifts between high and low density areas throughout the region, with very high densities in the southeastern portion in 2017 (Figure 7D), when lower numbers of false killer whales were present within the Hawaiian EEZ (Table 6). Yearly changes in the amount and location of higher density regions within the Hawaiian EEZ are also evident in the density maps for the larger central Pacific study area (Figure 7). These shifts in high- and low-density areas are more apparent when looking at maps specific to the Hawaiian EEZ, when in 2010 higher densities of false killer whales are predicted throughout much of the study area, particularly in the southern region, and lowest density regions are more constricted (Figure 9C). In contrast, the areas of predicted lowest density were larger and more prevalent in 2002 and 2017 (Figure 9B and D), and the areas of predicted high density in those years occurred more in patches, with particularly patchy high-density areas near the NWHI during 2002. The lowest predicted density in 2002 is within a region along the northern border of the Hawaiian EEZ between about 169°W and 174°W and 27°N and 29°N (Figure 9B), whereas in 2010 this region has some of the highest predicted densities (Figure 9C). In all years, there is a persistent area of predicted high density within the lee of the MHI and of predicted low density just south of Hawaiʻi Island, but the extent varies from year to year (Figure 9).

Comparison of Estimates

The average density and abundance of pelagic false killer whales in the Hawaiian EEZ across the period 2002 to 2017 estimated by the design-based approach (0.11 individuals 100 km^{-2} and 2,736 individuals; Table 5) is similar in magnitude to the estimate by the model-based approach (0.09 individuals 100 km^{-2} and 2,115 individuals; Table 6). Annual density and abundance estimates are more variable between the approaches, but do have overlapping 95% CIs for each HICEAS year (Tables 5−6; Figure 10).

Discussion

The present study is based on the most comprehensive line-transect survey dataset available to date for estimating the abundance of false killer whales within the Hawaiian EEZ and the broader central Pacific. Design- and model-based methodologies were combined to gain an understanding of a variety of ecological and sampling processes (e.g., habitat associations, animal movements, sampling variation, and potential biases). Taken together, these analyses meet multiple objectives, including (1) providing new 2017 and updated 2010 and 2002 estimates of false killer whale abundance within the Hawaiian EEZ for the NWHI and pelagic populations, (2) increasing the precision of abundance estimates for the pelagic population in all HICEAS years by using model-based methods while ensuring that the model-based estimates are unbiased compared to estimates from the design-based approach, and (3) estimating the abundance of pelagic false killer whales beyond the jurisdictional boundary of the EEZ to aid in managing U.S. and foreign longline fisheries and other human-caused factors impacting this population on the high seas.

Synthesis of Pelagic False Killer Whale Abundance Estimates

The comprehensive and careful consideration of all data collected from false killer whales during ship-based surveys in the central Pacific since 1986 has allowed for the application of two complementary, but analytically different approaches to estimating density and abundance for the pelagic population. The design- and model-based estimates of density and abundance in the Hawaiian EEZ (Tables 5−6), each averaged across years, provide broadly similar results, corroborating the outcome of each approach. The annual design-based estimates are highly variable, with the 2002 estimates nearly four times lower than the corresponding model-based estimates, the 2017 estimates more than double the model-based estimates, and the 2010 estimates nearly identical. The variability in the design-based estimates is likely largely due to the high encounter rate variance common when estimating the density of a rare species in a single year (e.g., Moore and Barlow 2014). In contrast, the model-based approach used the larger central Pacific false killer whale sighting dataset to derive relationships between habitat variables and false killer whale occurrence. These habitat associations, if adequately parameterized, can serve to smooth across annual variation in observed encounter rates, resulting in less variability between years. Much of the remaining variance can be attributed to environmental variability rather than to low single year sample size (Barlow et al. 2009; Forney et al. 2012).

While an SDM can minimize the effect of annual sampling variability, the implicit assumptions are that the habitat associations do not vary over time and that there are no underlying temporal trends in abundance aside from those predicted by changes in the environment. Population trends can be explicitly captured by an SDM by including a year term in the model (e.g., Becker et al. 2016), but more years of data, larger sample sizes, and potentially more information on factors affecting abundance are required than are currently available for pelagic false killer whales. Given the current sample size of the pelagic false killer whale SDM, annual trends and sampling variability are confounded, precluding use of a temporal trend effect. A simulation study was conducted to examine the role of random variation in encounter rate in the observed variation in the design-based estimates if pelagic false killer whale abundance in the Hawaiian EEZ did not vary substantially among years as suggested by the model-based approach (Appendix H). The simulated probability of drawing a value as low as or lower than the 2002 encounter rate by

chance was relatively small (6.6%). The probability of drawing a value as high as or higher than the 2017 encounter rate by chance was somewhat higher (12.8%). While these probabilities were fairly low overall, both the 2002 and 2017 encounter rates are plausible given random sampling variation and a constant abundance. Therefore, pronounced changes in the abundance of false killer whales in the Hawaiian EEZ is not a necessary condition to explain the differences in the design-based estimates.

Despite the limited number of available sightings, the SDM described false killer whale distribution patterns that are consistent with prior efforts to examine density and distribution for the species. Ferguson and Barlow (2003), using a similar model-based approach, estimated the highest densities of false killer whales at low latitudes in the eastern tropical Pacific, with a drop in density by an order of magnitude north of approximately 15°N. Forney et al. (2015), using a subset of the data available here, estimated density in the central Pacific to be an order of magnitude higher near the equator and south of the Hawaiian Islands than within the Hawaiian EEZ. The ability of the model-based analyses to capture the distributional differences is notable given the relatively small number of sightings within the southern portion of the central Pacific study area compared to the data available from the Hawaiian EEZ (Figure 2). The distributional patterns are also consistent with other data sources, including the distribution of false killer whales bycaught by Hawaii-based longline fisheries. Although the tuna-targeting longline fishery has generally shifted north and eastward since the mid to late-2000s (Woodworth-Jefcoats et al. 2018), false killer whale take rates in the decade prior to the shift were more than four times greater in the EEZ of Palmyra Atoll (located at 5°N) compared to the Hawaiian EEZ (Forney and Kobayashi 2007).

The SDM captured two aspects of false killer whale distribution that can affect the abundance of animals and the precision of design-based estimates within the Hawaiian EEZ study area. First, the predicted shifts in distribution between high- and low-density areas throughout the central Pacific study area (Figure 7) suggest there is some variation in the total number of animals within the Hawaiian EEZ in any given year. The year with the lowest model-based abundance estimate within the Hawaiian EEZ (2017) also had the greatest model-predicted densities along the equator and in the southeastern portion of the central Pacific study area (Figure 7D), perhaps suggesting that habitat was more favorable in those southern areas. Thus, habitat variation within the broader central Pacific could have contributed to at least some of the interannual variation in the design-based abundance estimates (Table 5). Second, the SDM captured changes in the patchiness of high-density areas, which would be expected to affect the precision of design-based estimates, since greater patchiness tends to lead to greater sampling variation. In general, the areas of predicted high density occurred more in patches in 2002 and 2017, when the number of sightings was somewhat lower and higher, respectively, than would have been expected if overall abundance was unchanged (Appendix H). There were also small but pronounced density patches in the NWHI in 2002. The resulting design-based CVs reflect this greater sampling uncertainty in 2002, when there was pronounced patchiness and only a single on-effort sighting was made. Combined, these factors suggest that at least some of the variation in design-based abundance estimates is attributable to spatial processes in animal distribution rather than true population changes.

A consideration of spatial processes is likewise relevant when interpreting differences in annual model-based density and abundance in the central Pacific study area. Although this region is

large geographically, the complete range of Hawai'i pelagic false killer whales, as well as those of other adjacent populations, is not known, such that habitat variation and movements of animals would be expected to influence the total number of animals present in a given year. Finally, the SDM estimated the average abundance in the central Pacific and Hawaiian EEZ study areas within and across the summer and fall survey period of each HICEAS year. These estimates may not be representative of pelagic false killer whale abundance during the winter and spring of 2002, 2010, and 2017, depending on the environmental conditions.

Influence of Data Collection Protocols and Parameter Estimates

Data collection for false killer whales during SWFSC and PIFSC ship-based line-transect surveys of the central Pacific has changed notably over the course of the three HICEAS efforts. The PC protocol used during PIFSC surveys starting in 2011 and in place during HICEAS 2017 allows for subgroup-based data collection that is compatible with line-transect density estimation. However, the standard closing mode group approaches during HICEAS 2002 and other surveys before HICEAS 2010 underestimated total group size because the relatively limited duration and spatial extent indicates that not all subgroups were accounted for in the estimate (Baird et al. 2008). This underestimation of group size likely led to a downward bias in the design-based estimates for 2002, as not all subgroups were accounted for in the estimate of expected number of subgroups.

The group-size estimation protocol implemented during HICEAS 2010 was developed to estimate group size more accurately by accounting for all associated subgroups. However, the protocol was difficult to successfully execute and was ultimately incompatible with the line-transect theoretical framework (Bradford et al. 2014). While the group-size estimation protocol used during HICEAS 2010 did account for additional subgroups, it is unknown which subgroups would actually have been detected had the PC protocol been implemented. Therefore, the probabilistic detections that form the basis of the encounter rate are a source of bias in the 2010 design-based estimates for NWHI and pelagic false killer whales, although the magnitude and direction are unknown. Additionally, three 2010 pelagic sightings were made of single, small subgroups (MII-098, MII-103, and MII-231; Table 2) while acoustics was off-effort and thus with a standard closing approach instead of the group-size estimation protocol. Consequently, additional subgroups may have been detected if the ship had stayed in passing mode.

The design-based abundance estimates were based on estimates of subgroup size, which match the unit of detection and were estimated using the PC protocol in the more recent surveys. In contrast, the SDM was based on additional data from years without the PC protocol, and statistical considerations required use of effective group size (number of detected subgroups times the average subgroup size) within the model to avoid overdispersion. Further, the inputs for the effective group sizes were linked to the design-based approach and thus based on a smaller truncation distance. The effect of these constraints on the accuracy and precision of the model-based abundance estimates is unknown. However, the similarity of the average abundance estimates within the Hawaiian EEZ for the design-based and model-based estimates suggests that any potential biases are likely relatively small. Further, the results of the encounter rate only model (Appendix E) show similar distribution patterns to those in the complete density models, indicating that bias from early data collection protocols and the use of uncertain effective group sizes did not significantly impact the model-based estimates.

The *g*(0) values used in this study (Table 3) are the greatest contributor to the increased abundance estimates relative to prior analyses of false killer whale abundance in the Hawaiian EEZ. Both the design- and model-based approaches resulted in higher abundance estimates for the Hawaiian EEZ than have been previously reported, with new design-based estimates nearly twice the prior estimates for HICEAS 2002 and HICEAS 2010 (Barlow and Rankin 2007; Bradford et al. 2014; Bradford et al. 2015). The updated analysis of *g*(0) indicates that prior estimates for this parameter were significantly underestimated, similar to most other cetacean species for which the same Beaufort-specific analysis has been undertaken (Barlow 2015). Although lower *g(0)* estimates explain the magnitude of increase in false killer whale abundance estimates relative to prior efforts (e.g., Bradford et al. 2014; Forney et al. 2015), the updated *g*(0) values were applied in both the design- and model-based approaches used here, reducing the influence of that parameter on the variation in the abundance resulting from each approach. The *g*(0) analysis used sightings from the central and eastern tropical Pacific to achieve an adequate sample across all Beaufort sea states. It is possible that behavioral or ecological factors differ between these areas and such differences cannot currently be accounted for with the available sample size. Estimation of Beaufort-specific *g*(0) for the central Pacific may be warranted as additional data are collected from this region. Additionally, the *g*(0) analysis used sightings at the group level because the change in encounter rate that would have resulted from including subgroups sighted in more recent years would likely have biased the results. The Beaufort-specific *g*(0) estimation could be transitioned to a subgroup-based analysis once more sightings made using the PC protocol are available. Similarly, an analysis of trackline detection probability using passive acoustic detection of subgroups could also be carried out to validate the Beaufort-specific values presented here. Such analysis was not feasible as part of this effort, as the tools for acoustically localizing and tracking false killer whales for comparison to visually observed subgroups require additional development. Despite these uncertainties, the Beaufort-specific *g*(0) values for false killer whales are generally in agreement with previous values estimated for large delphinids, such as bottlenose dolphins (Barlow 2015).

The prorated stock assignments used to estimate encounter rate are a source of potential bias in the abundance estimates within both analytical frameworks and for both populations. Ship-based sightings in areas of population overlap were used to determine proration values, but only a limited number of sightings of known population are available. There is a large amount of small-boat based sighting and telemetry data of known population that could be evaluated to estimate more precise proration values within the MHI-pelagic population overlap area (e.g., Baird et al. 2012). However, these data were not collected within the same framework and with the same constraints as the shipboard data, and developing a statistical approach to estimate proration values that could be applied to the ship-based sightings was beyond the scope of this study. Further, only ship-based sightings are available in the NWHI-pelagic population overlap area. While the estimated proration values may be a biased representation of the true relative abundance and sighting probability of each population, the abundance estimates are not sensitive to small deviations in the proration values. In contrast, the need for prorated values introduces bias within both frameworks and for both populations. Only a single prorated sighting from 2017 was used in the design-based estimation, such that the magnitude of the bias in the associated pelagic population estimate is likely small. However, the bias is more significant for the NWHI population because it is the only sighting used to estimate the abundance of that population in 2017. Approximately one third of the sightings used in the model-based estimation are of prorated sightings from the NWHI-pelagic and MHI-pelagic population overlap areas. The

model therefore used prorated values of encounter rate (i.e., a fractional sighting value for a segment with a prorated sighting) and when deriving the effective group size. The impact of using these prorated values within the model-based framework cannot be explicitly evaluated given the limited number of sightings that would be available for sensitivity analyses. However, the use of habitat covariates in the encounter rate and effective group size models likely mitigated the possible influence of sightings that were inappropriately allocated toward the pelagic population. Prior central Pacific models using all available false killer whale sightings, including those from the NWHI and MHI populations, did not select distance to land or depth as important variables (Forney et al. 2015), suggesting the model was driven by the habitat-associations of pelagic false killer whales throughout the broader study area.

The updated detection function from the design-based analysis is based on subgroup sightings that are overrepresented close to the trackline (Figure 2), which is suggestive of false killer whale movement toward the ship prior to detection by the visual observers. Although the model-based approach did not estimate a detection function explicitly, it relied on *ESW* values derived from the Beaufort-specific $g(0)$ analyses, which did require estimating a detection function. As in Bradford et al. (2014), the effect of likely vessel-attraction is minimized in the design and model-based approaches through the use of the half-normal model in the detection function, though it is likely that the resulting abundance estimates in all years are positively biased to some degree because of vessel attraction. The magnitude of vessel attraction and development of other analytical approaches to reducing this bias are underway using the towed hydrophone array detections of false killer whale subgroups.

Overview of NWHI False Killer Whale Abundance

The design-based abundance estimates for the NWHI population in 2010 and 2017 are similar (Table 5). While the point estimate is lower in 2017 than in 2010, the CV is higher, with the associated 95% CIs overlapping almost completely. As in Bradford et al. (2014), the NWHI abundance estimates remain difficult to interpret, not only because of their imprecision, but also because of how they are being affected by insular-type social structure and uncertainty in the current stock boundary (Bradford et al. 2015). Additional survey effort in the NWHI will be required to better understand the ecological associations of the NWHI population and the differential use of available habitat by each of the populations in that region.

Improvement in the Model-based Approach

The false killer whale SDM developed in this study is an improvement over previous efforts (Becker et al. 2012; Forney et al. 2015) because it more accurately accounts for variation in detection probabilities, corrects for lower $g(0)$ values in higher sea states, provides finer-scale density predictions (~9 km × 9 km grid resolution), includes additional years of survey data, and is specific to the pelagic population. Unlike the previous efforts that included sightings from the eastern tropical Pacific to increase sample size, the new model is specific to the central Pacific and Hawaiian EEZ study areas. The Forney et al. (2015) model was built with only 30 sightings and was simpler, including a null group size model and a single-predictor (SST) encounter rate model. Although the sample size in this study was only slightly larger (n = 38 sightings), the updated model identified relationships with dynamic habitat variables for both the encounter rate and group size models. The increased explanatory power may be a result of excluding survey data from the eastern tropical Pacific where habitat associations may differ. The sample size of

38 sightings used in the model-based approach is, however, still at the low end of what has been considered a suitable sample size for SDMs (Becker et al. 2010; Forney et al. 2015; Wisz et al. 2008). More sightings, particularly from outside the Hawaiian EEZ, could identify additional or changing habitat associations, facilitate the estimation of temporal and seasonal trends in abundance, and allow potential biases from input parameters to be evaluated through sensitivity analyses. Additional sighting data could also allow for model cross validation that was not possible given sample size limitations. In the future, it will be important to validate model predictions using either novel data (e.g., Becker et al. 2018) or data subsampling (e.g., Becker et al. 2010).

Similar to previous studies (Becker et al. 2012, Forney et al. 2015), the dynamic habitat predictors selected in the models are proxies for underlying (unmeasured) ecological processes. However, the inferred relationships appear to be consistent with known oceanographic features and species-habitat associations. For example, the encounter rate model included an interaction term between SSH and latitude. SSH provides an indication of mesoscale features such as eddies and fronts (Chelton et al. 2011). In the central Pacific study area, there are two prominent regions with such features, one along the equatorial fronts in tropical waters and the other in the North Pacific Transition Zone much farther north in temperate waters (Polovina and Howell 2005). These two regions are not the same ecologically, and the SSH:latitude interaction term allowed the model to treat these regions differently.

In conclusion, the combined use of design- and model-based approaches has led to a more integrated understanding of the density and abundance of false killer whales in the Hawaiian EEZ and broader central Pacific. There is utility in examining the results of both approaches within the context of different management requirements. Management applications that require spatially-explicit estimates of pelagic false killer whale density and abundance may now rely on robust population-specific estimates over the range of interest that incorporate all recent improvements in survey data collection and parameter estimation. The design-based estimates can be easily applied toward the computation of Potential Biological Removal (PBR), the metric against which human-caused impacts to the population are evaluated under the MMPA, for the Hawaiian EEZ, but the model-based abundance estimates provide a more stable temporal basis for managing pelagic false killer whales in this region and allow—for the first time—the estimation of total abundance and PBR within the entire central Pacific study area. Therefore, this approach can potentially be used to estimate the abundance of pelagic false killer whales within the entire fishing region of the Hawaii-based longline fleets known to interact with this population, providing a more robust method of managing fisheries impacts.

Acknowledgements

Literature Cited

Allouche O, Tsoar A, Kadmon R. 2006. Assessing the accuracy of species distribution models: prevalence, kappa and the true skill statistic (TSS). JAppl Ecol. 43(6):1223-1232.

Amante C, Eakins BW. 2009. ETOPO1 1 arc-minute global relief model: Procedures, data sources and analysis. U.S. Dep. Commer., NOAA Tech. Memo., NESDIS NGDC-24.

Baird RW. 2018. False killer whale: *Pseudorca crassidens*. In: Würsig B, Thewissen JGM, Kovacs KM, editors. Encyclopedia of marine mammals, 3rd edition. San Diego, CA: Academic Press. p. 347-349.

Baird RW, Schorr GS, Webster DL, McSweeney DJ, Hanson MB, Andrews RD. 2010. Movements and habitat use of satellite-tagged false killer whales around the main Hawaiian Islands. Endanger Species Res. 10:107-121.

Baird RW, Oleson EM, Barlow J, Ligon AD, Gorgone AM, Mahaffy SD. 2013. Evidence of an island-associated population of false killer whales (*Pseudorca crassidens*) in the Northwestern Hawaiian Islands. Pac Sci. 67(4):513-521.

Baird RW, Mahaffy SD, Gorgone AM, Cullins T, McSweeney DJ, Oleson EM, Bradford AL, Barlow J, Webster DL. 2015. False killer whales and fisheries interactions in Hawaiian waters: evidence for sex bias and variation among populations and social groups. Mar Mammal Sci. 31(2):579-590.

Baird RW, Gorgone AM, McSweeney DJ, Webster DL, Salden DR, Deakos MH, Ligon AD, Schorr GS, Barlow J, Mahaffy SD. 2008. False killer whales (*Pseudorca crassidens*) around the main Hawaiian Islands: long-term site fidelity, inter-island movements, and association patterns. Mar Mammal Sci. 24(3):591-612.

Baird RW, Hanson MB, Schorr GS, Webster DL, McSweeney DJ, Gorgone AM, Mahaffy SD, Holzer DM, Oleson EM, Andrews RD. 2012. Range and primary habitats of Hawaiian insular false killer whales: informing determination of critical habitat. Endanger Species Res. 18(1):47-61.

Barlow J. 1995. The abundance of cetaceans in California waters. Part I: ship surveys in summer and fall of 1991. Fish Bull. 93:1-14.

Barlow J. 2006. Cetacean abundance in Hawaiian waters estimated from a summer/fall survey in 2002. Mar Mammal Sci. 22(2):446-464.

Barlow J. 2015. Inferring trackline detection probabilities, g(0), for cetaceans from apparent densities in different survey conditions. Mar Mammal Sci. 31(3):923-943.

Barlow J, Rankin S. 2007. False killer whale abundance and density: preliminary estimates for the PICEAS study area south of Hawaii and new estimates for the US EEZ around Hawaii. Southwest Fisheries Science Center, Administrative Report LJ-07–02.

Barlow J, Gerrodette T, Forcada J. 2001. Factors affecting perpendicular sighting distances on shipboard line-transect surveys for cetaceans. J Cetacean Res Manag. 3(2):201-212.

Barlow J, Ferguson MC, Becker EA, Redfern JV, Forney KA, Vilchis IL, Fiedler PC, Gerrodette T, Ballance LT. 2009. Predictive modeling of cetacean densities in the eastern Pacific Ocean. U.S. Dep. Commer., NOAA Tech. Memo., NOAA-TM-NMFS-SWFSC-444.

Bates D, Machler M, Bolker BM, Walker SC. 2015. Fitting linear mixed-effects models using lme4. J Stat Softw. 67(1):1-48.

Bayless AR, Oleson EM, Baumann-Pickering S, Simonis AE, Marchetti J, Martin S, Wiggins SM. 2017. Acoustically monitoring the Hawai'i longline fishery for interactions with false killer whales. Fish Res. 190:122-131.

Becker EA, Forney KA, Foley DG, Barlow J. 2012. Density and spatial distribution patterns of cetaceans in the central North Pacific based on habitat models.: U.S. Dep. Commer., NOAA Tech. Memo., NOAA-TM-NMFS-SWFSC-490.

Becker EA, Forney KA, Foley DG, Smith RC, Moore TJ, Barlow J. 2014. Predicting seasonal density patterns of California cetaceans based on habitat models. Endanger Species Res. 23(1):1-22.

Becker EA, Forney KA, Ferguson MC, Foley DG, Smith RC, Barlow J, Redfern JV. 2010. Comparing California Current cetacean-habitat models developed using in situ and remotely sensed sea surface temperature data. Mar Ecol Prog Ser. 413:163-183.

Becker EA, Forney KA, Redfern JV, Barlow J, Jacox MG, Roberts JJ, Palacios DM. 2018. Predicting cetacean abundance and distribution in a changing climate. Divers Distrib. 25(4):626-643.

Becker EA, Forney KA, Fiedler PC, Barlow J, Chivers SJ, Edwards CA, Moore AM, Redfern JV. 2016. Moving towards dynamic ocean management: How well do modeled ocean products predict species distributions? Remote Sens-Basel. 8(2):149.

Bouchet PJ, Miller DL, Roberts JJ, Mannocci L, Harris CM, Thomas L. 2019. From here and now to there and then: Practical recommendations for extrapolating cetacean density surface models to novel conditions. Centre for Research into Ecological & Environmental Modelling (CREEM) Technical report 2019-01 v1.0.

Boyd C, Barlow J, Becker EA, Forney KA, Gerrodette T, Moore JE, Punt AE. 2018. Estimation of population size and trends for highly mobile species with dynamic spatial distributions. Divers Distrib. 24(1):1-12.

Bradford AL, Forney KA, Oleson EM, Barlow J. 2014. Accounting for subgroup structure in line-transect abundance estimates of false killer whales (*Pseudorca crassidens*) in Hawaiian waters. PLoS One. 9(2):e90464.

Bradford AL, Forney KA, Oleson EM, Barlow J. 2017. Abundance estimates of cetaceans from a line-transect survey within the U.S. Hawaiian Islands Exclusive Economic Zone. Fish Bull. 115:129-142.

Bradford AL, Oleson EM, Baird RW, Boggs CH, Forney KA, Young NC. 2015. Revised stock boundaries for false killer whales (*Pseudorca crassidens*) in Hawaiian waters. U.S. Dep. Commer., NOAA Tech. Memo., NOAA-TM-NMFS-PIFSC-47.

Bradford AL, Baird RW, Mahaffy SD, Gorgone AM, McSweeney DJ, Cullins T, Webster DL, Zerbini AN. 2018. Abundance estimates for management of endangered false killer whales in the main Hawaiian Islands. Endanger Species Res. 36:297-313.

Buckland ST, Anderson DR, Burnham KP, Laake JL, Borchers DL, Thomas L. 2001. Introduction to distance sampling. Estimating abundance of biological populations. Oxford, UK: Oxford University Press.

Carretta JV, Forney KA, Lowry MS, Barlow J, Baker J, Johnston D, Hanson B, Muto MM, Lynch D, Carswell L. 2009. U.S. Pacific marine mammal stock assessments: 2008. U.S. Dep. Commer., NOAA Tech. Memo., NOAA-TM-NMFS-SWFSC-434.

Carretta JV, Forney KA, Oleson EM, Weller DW, Lang AR, Baker J, Weller DW, Muto MM, Hanson B, Orr AJ et al. 2017. U.S. Pacific marine mammal stock assessments: 2016. U.S. Dep. Commer., NOAA Tech. Memo., NOAA-TM-NMFS-SWFSC-577.

Chelton DB, Schlax MG, Samelson RM. 2011. Global observations of nonlinear mesoscale eddies. Prog Oceanogr. 91(2):167-216.

Chivers SJ, Baird RW, McSweeney DJ, Webster DL, Hedrick NM, Salinas JC. 2007. Genetic variation and evidence for population structure in eastern North Pacific false killer whales (*Pseudorca crassidens*). Can J Zool. 85(7):783-794.

Chivers SJ, Baird RW, Martien KM, Taylor BL, Archer E, Gorgone AM, Hancock BL, Hedrick NM, Matilla D, McSweeney DJ et al. 2010. Evidence of genetic differentiation for Hawai'i insular false killer whales (*Pseudorca crassidens*). U.S. Dep. Commer., NOAA Tech. Memo., NOAA-TM-NMFS-SWFSC-458.

Douglas DC, Weinzierl R, Davidson SC, Kays R, Wikelski M, Bohrer G. 2012. Moderating Argos location errors in animal tracking data. Methods Ecol Evol. 3(6):999-1007.

Fawcett T. 2006. An introduction to ROC analysis. Pattern Recognition Letters. 27(8):861-874.

Ferguson MC, Barlow J. 2003. Addendum: Spatial distribution and density of cetaceans in the eastern tropical Pacific Ocean based on summer/fall research vessel surveys in 1986-96. Southwest Fisheries Science Center, Administrative Report LJ-01-04 (Addendum).

Forney KA. 2000. Environmental models of cetacean abundance: Reducing uncertainty in population trends. Conserv Biol. 14(5):1271-1286.

Forney KA, Kobayashi DR. 2007. Updated estimates of mortality and injury of cetaceans in the Hawaii-based longline fishery, 1994-2005. U.S. Dep. Commer., NOAA Tech. Memo., NOAA-TM-NMFS-SWFSC-412.

Forney KA, Kobayashi DR, Johnston DW, Marchetti JA, Marsik MG. 2011. What's the catch? Patterns of cetacean bycatch and depredation in Hawaii-based pelagic longline fisheries. Mar Ecol. 32(3):380-391.

Forney KA, Becker EA, Foley DG, Barlow J, Oleson EM. 2015. Habitat-based models of cetacean density and distribution in the central North Pacific. Endanger Species Res. 27(1):1-20.

Forney KA, Ferguson MC, Becker EA, Fiedler PC, Redfern JV, Barlow J, Vilchis IL, Ballance LT. 2012. Habitat-based spatial models of cetacean density in the eastern Pacific Ocean. Endanger Species Res. 16(2):113-133.

Gerrodette T, Forcada J. 2005. Non-recovery of two spotted and spinner dolphin populations in the eastern tropical Pacific Ocean. Mar Ecol Prog Ser. 291:1-21.

Guisan A, Thuiller W. 2005. Predicting species distribution: offering more than simple habitat models. Ecol Lett. 8(9):993-1009.

Hastie TJ, Tibshirani RJ. 1990. Generalized additive models. Boca Raton, USA: Chapman and Hall/CRC.

Hedley SL, Buckland ST. 2004. Spatial models for line transect sampling. J Agr Biol Envir St. 9(2):181-199.

Kinzey D, Olson P, Gerrodette T. 2000. Marine mammal data collection procedures on research ship line-transect surveys by the Southwest Fisheries Science Center. Southwest Fisheries Science Center, Administrative Report LJ-00-08.

Laake J, Borchers D, Thomas L, Miller D, Bishop J. 2018. Package 'mrds'. https://cran.r-project.org/web/packages/mrds/mrds.pdf. 2.2.0 ed.

Liu C, Berry PM, Dawson TP, Pearson RG. 2005. Selecting thresholds of occurrence in the prediction of species distributions. Ecography. 28(3):385-393.

Mann KH, Lazier JRN. 2005. Dynamics of marine ecosystems: Biological-physical interactions in the Oceans. Malden, USA: Blackwell Publishing.

Mannocci L, Monestiez P, Spitz J, Ridoux V. 2015. Extrapolating cetacean densities beyond surveyed regions: habitat-based predictions in the circumtropical belt. J Biogeogr. 42(7):1267-1280.

Marra G, Wood SN. 2011. Practical variable selection for generalized additive models. Comput Stat Data An. 55(7):2372-2387.

Martien KK, Chivers SJ, Baird RW, Archer FI, Gorgone AM, Hancock-Hanser BL, Mattila D, McSweeney DJ, Oleson EM, Palmer C et al. 2014. Nuclear and mitochondrial patterns of population structure in North Pacific false killer whales (*Pseudorca crassidens*). J Hered. 105(5):611-626.

Miller DL, Burt ML, Rexstad EA, Thomas L. 2013. Spatial models for distance sampling data: recent developments and future directions. Methods Ecol Evol. 4(11):1001-1010.

Moore J, Barlow J. 2017. Population abundance and trend estimates for beaked whales and sperm whales in the California Current from ship-based visual line-transect survey data, 1991-2014. U.S. Dep. Commer., NOAA Tech. Memo., NOAA-TM-NMFS-SWFSC-585.

Moore JE, Barlow JP. 2014. Improved abundance and trend estimates for sperm whales in the eastern North Pacific from Bayesian hierarchical modeling. Endanger Species Res. 25(2):141-150.

Oleson EM, Boggs CH, Forney KA, Hanson MB, Kobayashi DR, Taylor BL, Wade PR, Ylitalo GM. 2010. Status review of Hawaiian insular false killer whales (*Pseudorca crassidens*) under the Endangered Species Act. U.S. Dep. Commer., NOAA Tech. Memo., NOAA-TM-NMFS-PIFSC-22.

Palacios DM, Bailey H, Becker EA, Bograd SJ, DeAngelis ML, Forney KA, Hazen EL, Irvine LM, Mate BR. 2019. Ecological correlates of blue whale movement behavior and its predictability in the California Current Ecosystem during the summer-fall feeding season. Mov Ecol. 7:26.

Polovina JJ, Howell EA. 2005. Ecosystem indicators derived from satellite remotely sensed oceanographic data for the North Pacific. Ices J Mar Sci. 62(3):319-327.

R Core Team. 2017. R: a language and environment for statistical computing. R Foundation for Statistical Computing. Vienna, Austria.

R Core Team. 2019. R: a language and environment for statistical computing. R Foundation for Statistical Computing. Vienna, Austria.

Redfern JV, Moore TJ, Fiedler PC, de Vos A, Brownell RL, Forney KA, Becker EA, Ballance LT. 2017. Predicting cetacean distributions in data-poor marine ecosystems. Divers Distrib. 23(4):394-408.

Roberts JJ, Best BD, Mannocci L, Fujioka E, Halpin PN, Palka DL, Garrison LP, Mullin KD, Cole TV, Khan CB et al. 2016. Habitat-based cetacean density models for the U.S. Atlantic and Gulf of Mexico. Sci Rep. 6:22615.

Schwarz LK, Gerrodette T, Archer F. 2010. Comparison of closing and passing from a line-transect survey of delphinids in the eastern Tropical Pacific Ocean. J Cetacean Res Manag. 11(3):253-265.

Seber GAF. 1982. The estimation of animal abundance and related parameters. New York, USA: Macmillan.

Thomas L, Williams R, Sandilands D. 2007. Designing line transect surveys for complex regions. J Cetacean Res Manag. 9(1):1-13.

Thomas L, Buckland ST, Rexstad EA, Laake JL, Strindberg S, Hedley SL, Bishop JR, Marques TA, Burnham KP. 2010. Distance software: design and analysis of distance sampling surveys for estimating population size. J Appl Ecol. 47(1):5-14.

Wisz MS, Hijmans RJ, Li J, Peterson AT, Graham CH, Guisan A, Group NPSDW. 2008. Effects of sample size on the performance of species distribution models. Divers Distrib. 14(5):763-773.

Wood SN. 2003. Thin plate regression splines. J Roy Stat Soc B. 65:95-114.

Wood SN. 2008. Fast stable direct fitting and smoothness selection for generalized additive models. J Roy Stat Soc B. 70:495-518.

Wood SN. 2011. Fast stable restricted maximum likelihood and marginal likelihood estimation of semiparametric generalized linear models. J Roy Stat Soc B. 73:3-36.

Wood SN. 2017. Generalized additive models: An introduction with R. New York, USA: Chapman and Hall/CRC.

Woodworth-Jefcoats PA, Polovina JJ, Drazen JC. 2018. Synergy among oceanographic variability, fishery expansion, and longline catch composition in the central North Pacific Ocean. Fish Bull. 116(3-4):228-239.

Yano KM, Oleson EM, Keating JL, Ballance LT, Hill MC, Bradford AL, Allen AN, Joyce TW, Moore JE, Henry A. 2018. Cetacean and seabird data collected during the Hawaiian Islands Cetacean and Ecosystem Assessment Survey (HICEAS), July-December 2017. U.S. Dep. Commer., NOAA Tech. Memo., NOAA-TM-NMFS-PIFSC-72.

Yuan Y, Bachl FE, Lindgren F, Borchers DL, Illian JB, Buckland ST, Rue H, Gerrodette T. 2017. Point process models for spatio-temporal distance sampling data from a large-scale survey of blue whales. Ann Appl Stat. 11(4):2270-2297.

Tables

Table 1. Cetacean line-transect surveys conducted by the Southwest or Pacific Islands Fisheries Science Centers that focused on or transited through part of the central Pacific and had false killer whale sightings and effort data that were included in one or both of the density estimation approaches (design- or model-based).

Year	Survey Period	Survey No.	Focal Region	Approach Informed
1986	Jul – Dec	0989	Eastern tropical Pacific	Design
1986	Aug – Dec	0990	Eastern tropical Pacific	Design
1987	Jul – Dec	1080	Eastern tropical Pacific	Design
1989	Jul – Dec	1268	Eastern tropical Pacific	Design
1990	Jul – Dec	1370	Eastern tropical Pacific	Design
1997	Mar – Jun	1607	Temperate North Pacific	Model
1998	Jul – Dec	1611	Eastern tropical Pacific	Both
1999	Jul – Dec	1614	Eastern tropical Pacific	Both
2000	Jul – Dec	1616	Eastern tropical Pacific	Both
2002	Jul – Dec	1621	Hawaiian EEZ	Both
2002	Oct – Dec	1622	Hawaiian EEZ	Both
2005	Jul – Nov	1629	Central Pacific islands	Both
2006	Jul – Dec	1631	Eastern tropical Pacific	Both
2009	Feb	0901	Main Hawaiian Islands	Both
2010	Apr – May	1004	Central Pacific transit	Design
2010	Aug – Dec	1641	Hawaiian EEZ	Both
2010	Sep – Oct	1642	Hawaiian EEZ	Both
2011	Oct – Nov	1108	Palmyra Atoll	Both
2012	Apr – May	1203	Palmyra Atoll	Both
2013	May – Jun	1303	Northwestern Hawaiian Islands	Both
2016	Jun – Jul	1604	Main Hawaiian Islands	Both
2017	Aug – Dec	1705	Hawaiian EEZ	Both
2017	Jul – Oct	1706	Hawaiian EEZ	Both

Surveys were considered as informing the model-based approach if they were used in the encounter rate model (Appendix A). The Hawaiian Islands Cetacean Ecosystem and Assessment Surveys in 2002, 2010, and 2017 include two survey numbers (one for each survey vessel), and the survey period reflects all effort, including time outside the U.S. Exclusive Economic Zone of the Hawaiian Islands (Hawaiian EEZ).

Table 2. Details of the false killer whale sightings made on systematic survey effort during the Hawaiian Islands Cetacean Ecosystem and Assessment Survey (HICEAS) in 2002, 2010, and 2017.

HICEAS	Date	Sighting No.	Stratum	Population	Group Size	Phase 1_{TOT}	Phase 1_{EST}	n
2002	09/24/02	DSJ-184	Outer-EEZ	Pelagic	10.3	-	-	2.8
2010	09/01/10	MII-035	EEZ	Pelagic	22.6	-	-	3.1
2010	09/26/10	OES-086	EEZ	NWHI	52.0	-	-	4.6
2010	09/27/10	MII-098	EEZ	Pelagic	1.9	-	-	1.0
2010	09/28/10	MII-103	EEZ	Pelagic	1.0	-	-	1.0
2010	10/31/10	MII-231	EEZ	Pelagic	1.0	-	-	1.0
2010	11/10/10	MII-241	EEZ	Pelagic	41.0	-	-	6.4
2017	07/23/17	OES-033	EEZ	Pelagic	-	5	4	4.0
2017	07/24/17	OES-035	EEZ	Pelagic	-	1	0	0.0
2017	07/27/17	OES-039	EEZ	Pelagic	-	7	4	4.0
2017	09/13/17	OES-122	EEZ	Pelagic	-	5	3	3.0
2017	09/17/17	OES-133	EEZ	NWHI or pelagic	-	7	6	2.4 or 3.6[1]
2017	09/20/17	OES-141	EEZ	Pelagic	-	1	1	1.0
2017	09/21/17	LAS-064	EEZ	Pelagic	-	2	2	2.0
2017	09/29/17	LAS-073	EEZ	Pelagic	-	9	6	6.0
2017	10/08/17	OES-176	EEZ	MHI[2]	-	1	0	0.0

All sightings were made within the U.S. Exclusive Economic Zone (EEZ) of the Hawaiian Islands, but a main Hawaiian Islands (MHI) stratum was sampled more intensively in 2002. Sightings were assigned to either the MHI, Northwestern Hawaiian Islands (NWHI), or pelagic population based on photo-identification, genetic, movement, or sighting location relative to stock boundary (Figure 1). Phase 1_{TOT} is the number of subgroups sighted in Phase 1; Phase 1_{EST} is the number of subgroups appropriate to use for density estimation; and n is the number of subgroups (expected or actual) contributing to the encounter rate in the design-based density estimation for the NWHI and pelagic populations. See Appendix A for complete list of sightings used in the design- and model-based estimation.

[1]$n = 2.4$ for the NWHI population; $n = 3.6$ for the pelagic population.

[2]Line-transect abundance estimates were not pursued for the MHI population, as more precise estimates were made using mark-recapture methods (Bradford et al. 2018).

Table 3. Beaufort-specific estimates of trackline detection probability (*g*(0)) and effective strip width (*ESW*) for false killer whales in Beaufort sea states (*b*) 0−6 along with corresponding sighting sample size (n).

Parameter	*b*0	*b*1	*b*2	*b*3	*b*4	*b*5	*b*6
n	4	5	12	25	41	22	4
g(0)	1.00	1.00	0.72	0.51	0.37	0.26	0.19
g(0) CV	0.00	0.00	0.11	0.22	0.34	0.46	0.59
ESW (km)	3.64	3.37	3.10	2.82	2.56	2.30	2.07
ESW CV	0.23	0.19	0.14	0.07	0.07	0.15	0.24

Detection probabilities in Beaufort states of 0 and 1 are assumed to be certain (*g*(0)=1), and relative probabilities in other conditions are estimated from a model that assumes that true group densities are independent of Beaufort when time and location effects are removed (Barlow 2015).

Table 4. Estimates of line-transect parameters and associated details used to produce stratum-specific design-based abundance estimates of false killer whales of the Northwestern Hawaiian Islands (NWHI) and pelagic populations during the Hawaiian Islands Cetacean Ecosystem and Assessment Survey in 2002, 2010, and 2017.

Population	Year	Stratum	*g*(0)	CV	n_{ij}	L_{ij}	No. Effort Segments	n_{ij}/L_{ij}	CV
NWHI	2010	EEZ	0.40	0.29	4.6	2,838[1]	25	0.17	1.03
	2017	EEZ	0.37	0.30	2.4	2,977	28	0.08	1.56
Pelagic	2002	Outer-EEZ	0.37	0.31	2.8	13,473	99	0.02	1.06
	2010	EEZ	0.37	0.32	12.5	16,192[1]	114	0.08	0.59
	2017	EEZ	0.34	0.34	23.6	16,209	113	0.15	0.42

A main Hawaiian Islands (MHI) stratum was sampled more intensively within the U.S. Exclusive Economic Zone (EEZ) of the Hawaiian Islands in 2002, although no false killer whales were sighted there. The length of surveyed transects is shown in km, and the subgroup encounter rate (n_{ij}/L_{ij}) is presented in subgroups 100 km^{-1}. See text for remaining details of the parameters.

[1]Includes the length of the on-effort projected trackline.

Table 5. Design-based estimates of density (individuals 100 km^{-2}) and abundance of false killer whales in the Northwestern Hawaiian Islands (NWHI) and pelagic populations in each applicable year of the Hawaiian Islands Cetacean Ecosystem and Assessment Survey (2002, 2010, and 2017) and averaged over all years.

Population	Year	Density	Abundance	CV	95% CI
NWHI	2010	0.20	878	1.15	145–5,329
	2017	0.11	477	1.71	48–4,712
	Average	0.15	678	1.12	116–3,950
Pelagic	2002	0.03	613	1.20	96–3,906
	2010	0.10	2,489	0.74	678–9,143
	2017	0.21	5,106	0.63	1,640–15,892
	Average	0.11	2,736	0.53	1,030–7,269

Table 6. Model-predicted estimates of density (individuals 100 km^{-2}) and abundance of pelagic false killer whales in the central Pacific and U.S. Exclusive Economic Zone of the Hawaiian Islands (Hawaiian EEZ) study areas for 2002, 2010, 2017, as well as the multiyear average estimates.

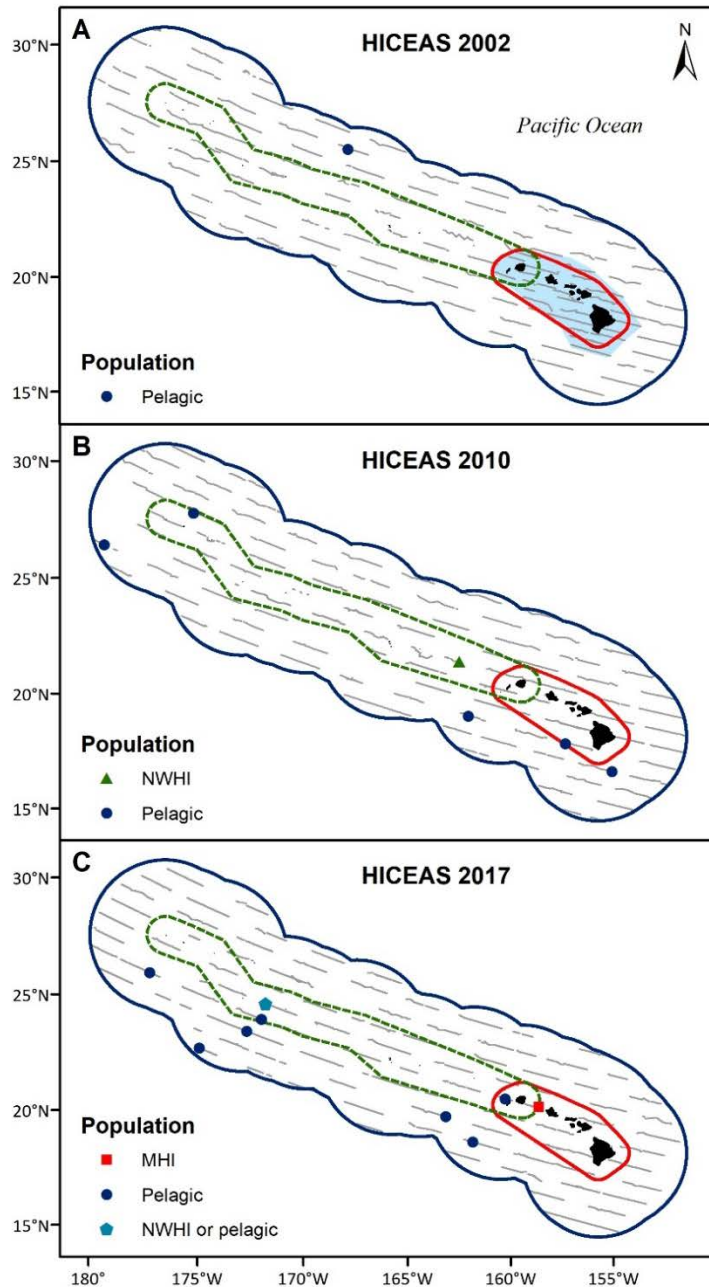|	Central Pacific				Hawaiian EEZ			
Year	Density	Abundance	CV	95% CI	Density	Abundance	CV	95% CI
2002	0.10	25,723	0.30	14,397–45,958	0.09	2,122	0.33	1,136–3,964
2010	0.10	25,212	0.33	13,449–47,262	0.09	2,144	0.32	1,159–3,965
2017	0.13	34,536	0.35	17,857–66,792	0.09	2,086	0.35	1,079–4,031
Average	0.11	29,291	0.32	15,782–54,363	0.09	2,115	0.34	1,111–4,026

Figures

Figure 1. Locations of false killer whale groups sighted during systematic line-transect survey effort (fine lines) in Beaufort sea states 0−6 within the U.S. Hawaiian Islands Exclusive Economic Zone (blue outline) during the Hawaiian Islands Cetacean Ecosystem and Assessment Survey (HICEAS) in (A) 2002, (B) 2010, and (C) 2017.

The sighting markers are differentiated by population; either main Hawaiian Islands (MHI), Northwestern Hawaiian Islands (NWHI), pelagic, or unknown as shown in the legend. The solid red and dashed green lines represent the MHI and NWHI stock boundaries, respectively (Bradford et al. 2015). The light blue polygon represents the MHI survey stratum used during HICEAS 2002. The MHI are shown in black.
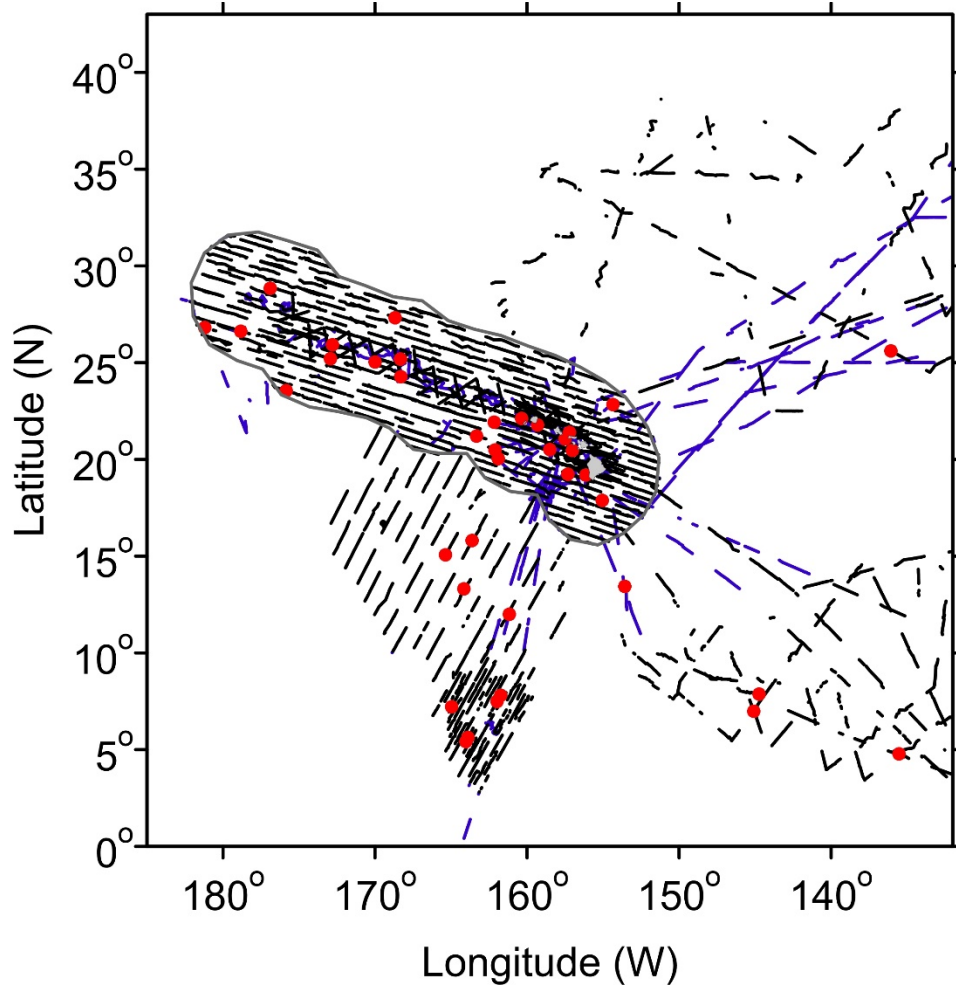
Figure 2. Locations of pelagic false killer whale sightings (n = 38, red dots) made while on-effort during line-transect surveys in Beaufort sea states 0−6 within the central Pacific study area used in the model-based approach.

Effort from both systematic (black lines) and nonsystematic (blue lines) transects were used in the habitat model. The U.S. Hawaiian Islands Exclusive Economic Zone is outlined in gray.
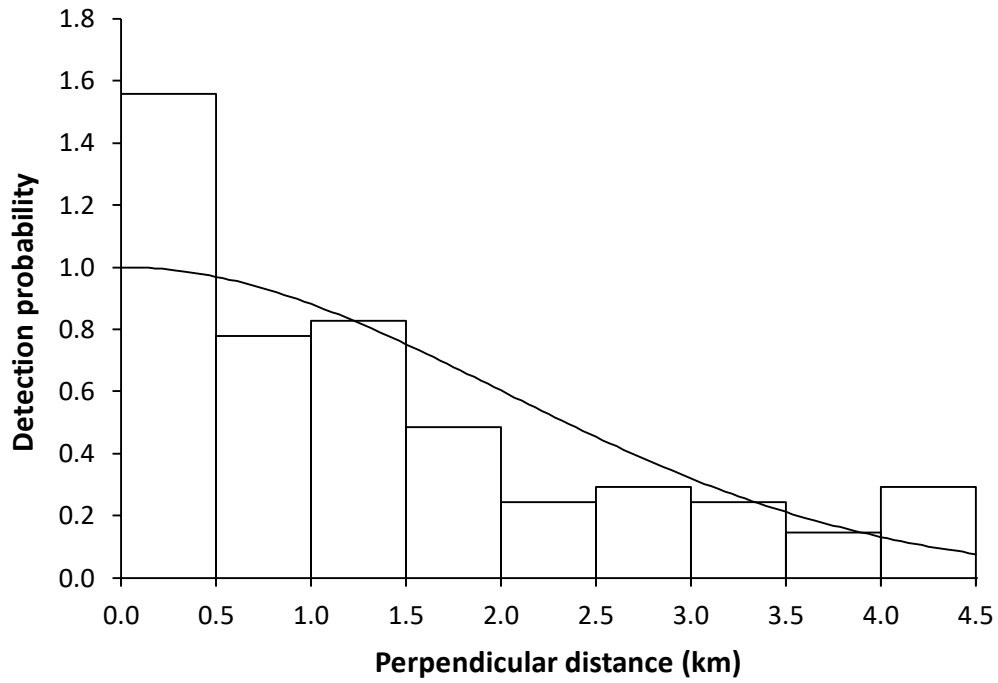
Figure 3. Histogram of systematic and nonsystematic survey effort false killer whale subgroup sightings (n = 100) by perpendicular distance from the trackline and fit of the half-normal model used to estimate the detection function of subgroups used in the design-based approach.
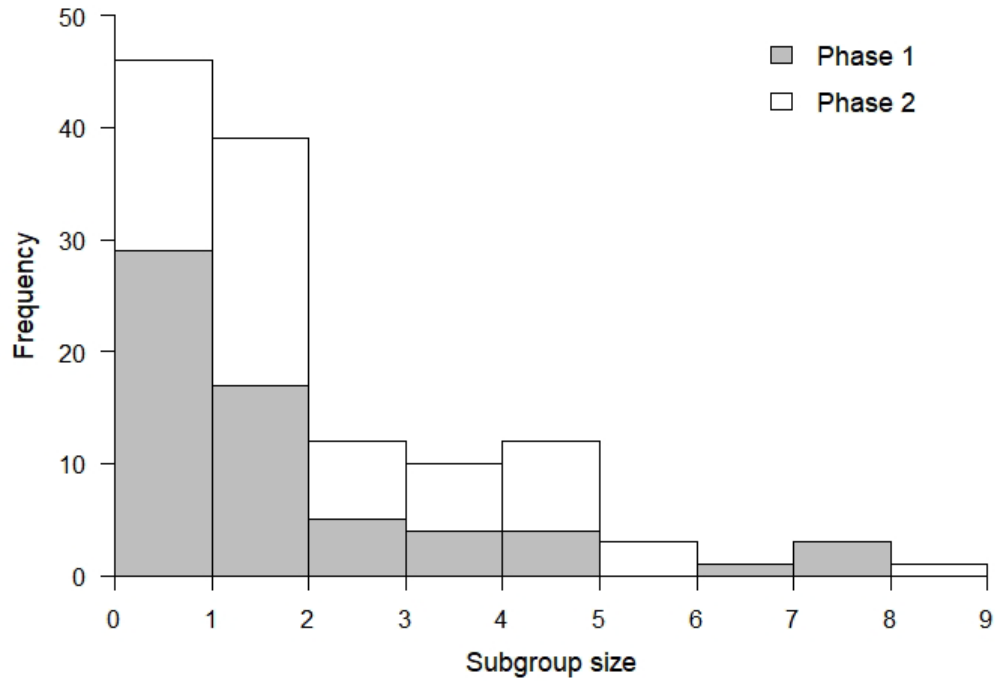
Figure 4. Frequency of false killer whale subgroup sizes used in the estimation of expected subgroup size.

Subgroup sizes were made during phase 1 (n = 63) and phase 2 (n = 64) of the PC protocol implemented during line-transect surveys conducted by the Pacific Islands Fisheries Science Center between 2011 and 2017.
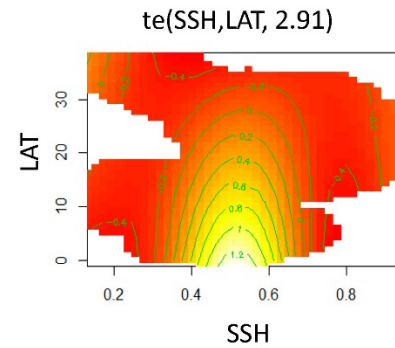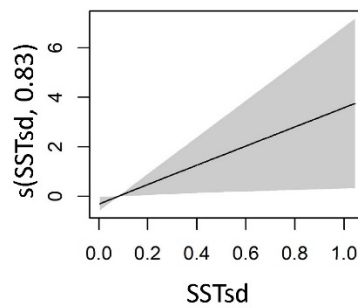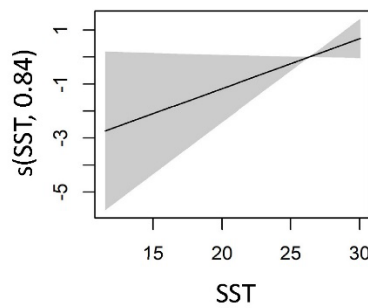
Figure 5. Functional forms for habitat variables included in the final (A) group size and (B) encounter rate models of pelagic false killer whales in the central Pacific study area.

Variables included mixed layer depth (MLD), sea surface temperature (SST), standard deviation of SST (SSTsd), and a bivariate sm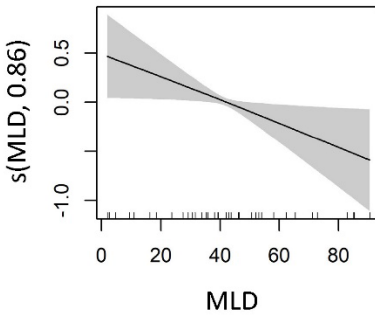ooth of sea surface height (SSH) and latitude (LAT) (north latitudes). The y-axes represent the term's (linear or spline) function, with the degrees of freedom shown in parentheses on the y-axis (linear terms are represented by a single degree of freedom). Zero on the y-axes corresponds to no effect of the predictor variable on the estimated response variable. Scaling of y-axis varies among predictor variables to emphasize model fit. The shading reflects 2× standard error bands (i.e., 95% confidence interval); tick marks ('rug plot') in the group size model above the x-axis show data values. Contour values in the bivariate smooth indicate the influence of the smooth (red=low, yellow=high).
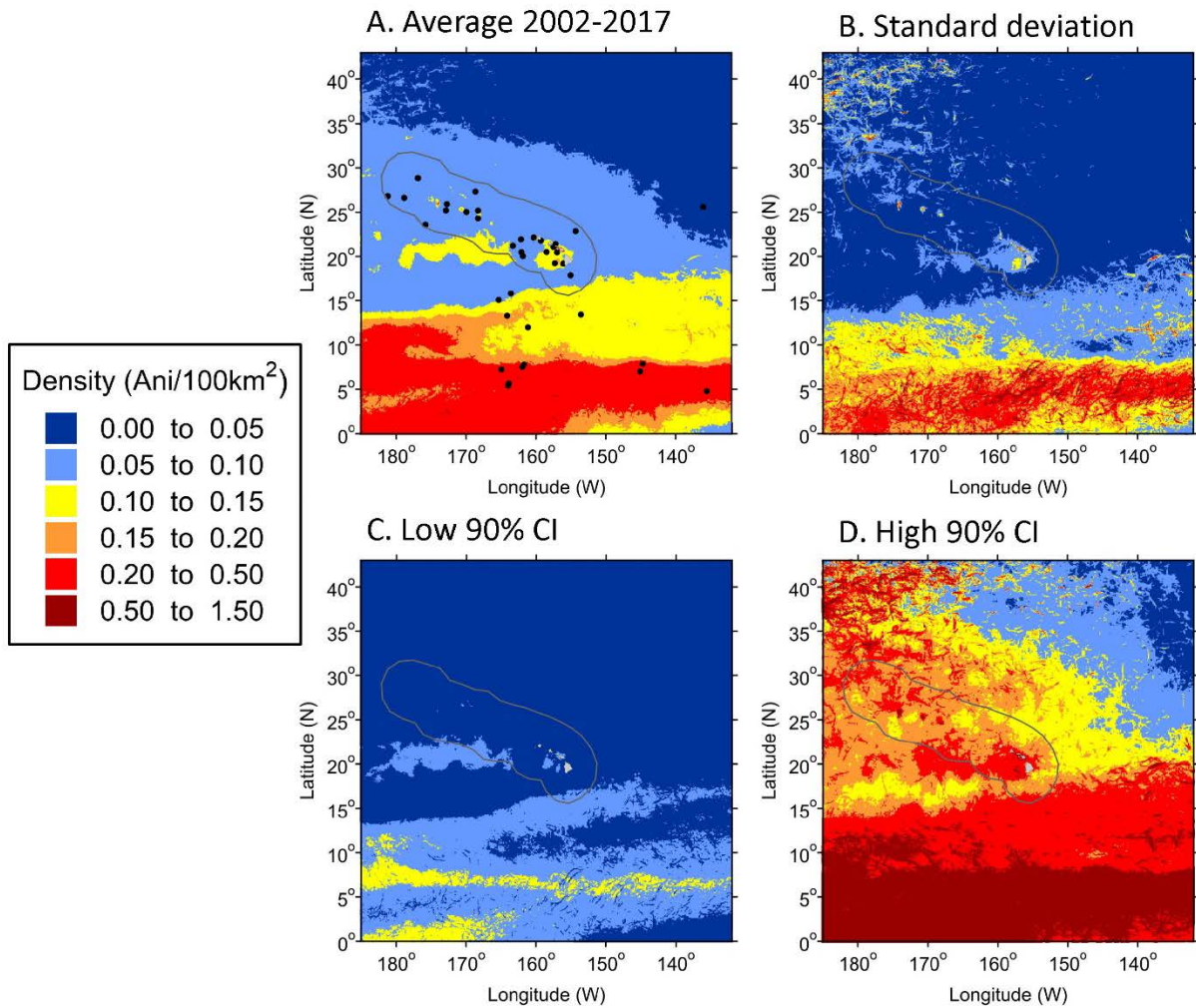
Figure 6. Predicted densities and uncertainty from the habitat-based density model for pelagic false killer whales in the central Pacific study area, showing (A) the multi-year (2002, 2010, and 2017) average, (B) the standard deviation of density, (C) the lower 90% confidence interval (Low 90% CI) and (D) the upper 90% confidence interval (High 90% CI).

Density ranges are defined by linear increments and encompass all values within the confidence limits. The black dots in the multi-year average map show the pelagic false killer whale sighting locations (n = 38) from 1997 to 2017 used to develop the habitat models. The U.S. Hawaiian Islands Exclusive Economic Zone is outlined in gray.

Figure 7. Predicted densities from the habitat-based density model for pelagic false killer whales in the central Pacific study area based on tri-daily predictions averaged across (A) all years (2002, 2010, and 2017), (B) 2002, (C) 2010, and (D) 2017 (see text for details).

Density ranges are defined by linear increments specific to the average and used in the yearly plots for comparison. The black dots in the multi-year average show the pelagic false killer whale sighting locations (n = 38) from 1997 to 2017 used to develop the habitat models. The U.S. Hawaiian Islands Exclusive Economic Zone is outlined in gray.
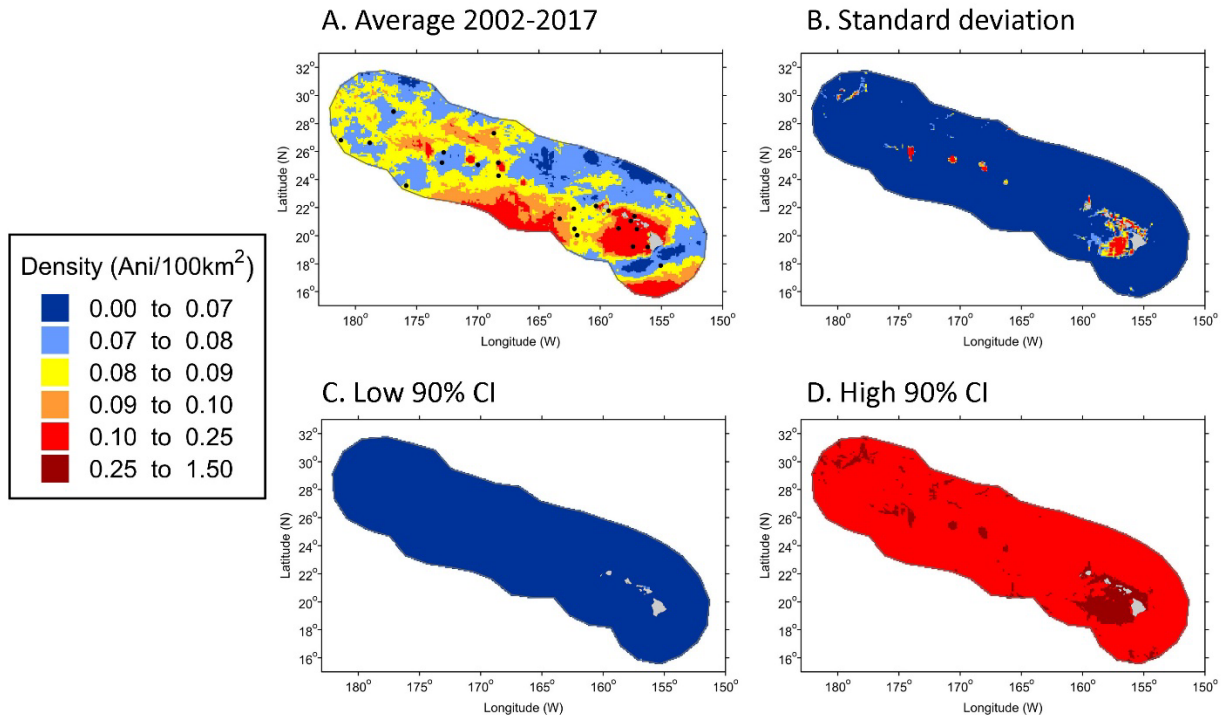
Figure 8. Predicted densities and uncertainty for the U.S. Hawaiian Islands Exclusive Economic Zone (Hawaiian EEZ) study area from the habitat-based density model for pelagic false killer whales in the central Pacific study area, showing (A) the multi-year (2002, 2010, and 2017) average, (B) the standard deviation of density, (C) the lower 90% confidence interval (Low 90% CI) and (D) the upper 90% confidence interval (High 90% CI).

Density ranges are defined by linear increments and encompass all values within the confidence limits. The range in density values is specific to the Hawaiian EEZ to show variability within this smaller study area. The black dots in the multi-year average plot show the pelagic false killer whale sighting locations (n = 38) from 1997 to 2017.

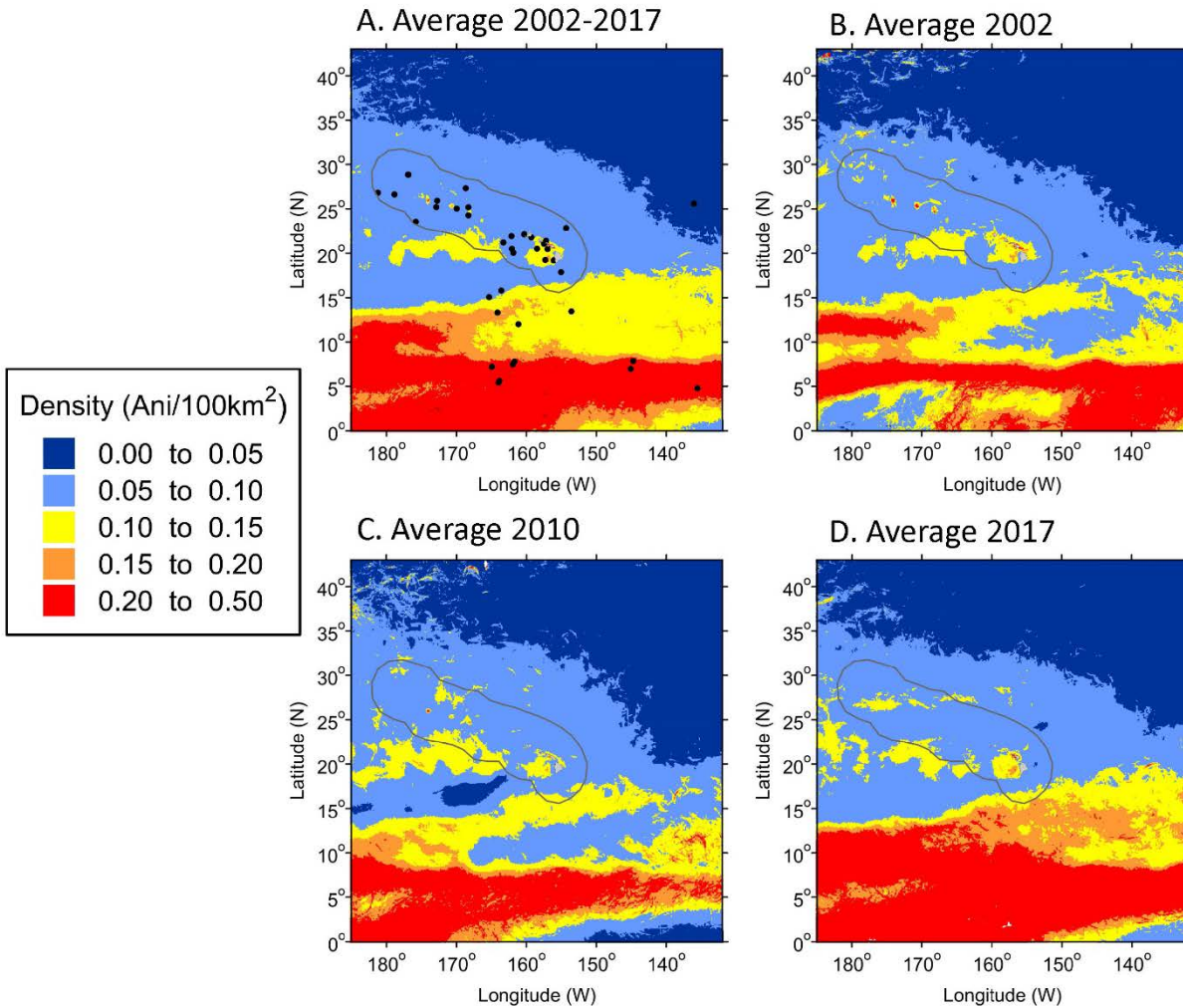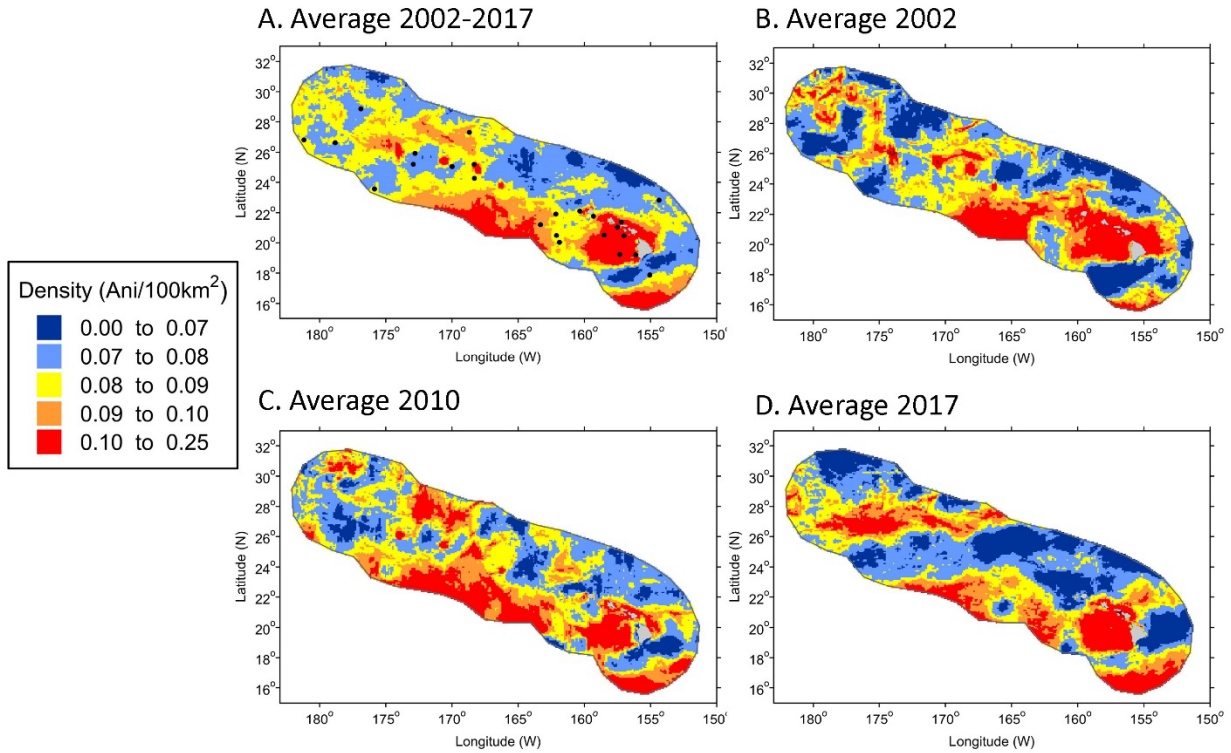**Figure 9. Predicted densities for the U.S. Hawaiian Islands Exclusive Economic Zone (Hawaiian EEZ) study area from the habitat-based density model for pelagic false killer whales in the central Pacific study area based on tri-daily predictions averaged across (A) all years (2002, 2010, and 2017), (B) 2002, (C) 2010, and (D) 2017 (see text for details).**

Density ranges are defined by linear increments specific to the average and used in the yearly plots for comparison. The range of density values is specific to the Hawaiian EEZ in order to show variability within this smaller study area. The black dots in the multi-year average plot show the false killer whale sighting locations (n = 38) from 1997 to 2017.
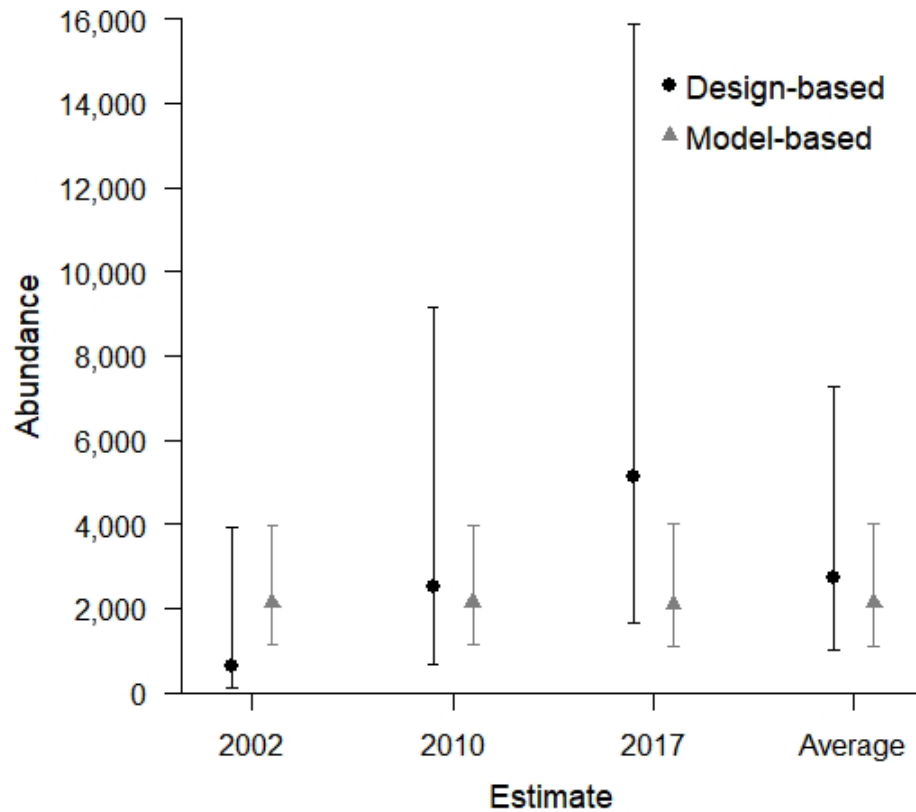
Figure 10. Design- and model-based abundance estimates of pelagic false killer whales in the U.S. Exclusive Economic Zone of the Hawaiian Islands for each year of the Hawaiian Islands Cetacean and Ecosystem Assessment Survey (HICEAS; 2002, 2010, and 2017) and averaged over all HICEAS years.

Appendix A: Analysis Sightings of False Killer Whales

Table A 1. Sightings of false killer whales (n = 79) from line-transect surveys of the central Pacific between 1986 and 2017 used in the density estimation. Table continues on following two pages, and notes follow end of table.

| Year	Survey No.	Sighting No.[1]	Effort	Population	$f(0)$	$E(s)$	$g(0)^2$	n/L – Design	n/L – Model	n Pelagic
1986	0989	DSJ-001-1128	S	Pelagic	-	-	✓	-	-	-
1986	0990	MAC-002-1113	S	Pelagic	✓	-	✓	-	-	-
1987	1080	MAC-005-0819	S	Pelagic	✓	-	✓	-	-	-
1987	1080	MAC-003-0909	S	Pelagic	-	-	✓	-	-	-
1987	1080	MAC-001-1128	S	Pelagic	-	-	✓	-	-	-
1987	1080	MAC-001-1201	S	Pelagic	✓	-	✓	-	-	-
1989	1268	MAC-001-0822	S	Pelagic	✓	-	✓	-	-	-
1989	1268	MAC-003-0822	S	Pelagic	✓	-	✓	-	-	-
1989	1268	MAC-009-0910	S	Pelagic	✓	-	✓	-	-	-
1990	1370	MAC-004-0822	S	Pelagic	-	-	✓	-	-	-
1990	1370	MAC-001-0909	S	Pelagic	✓	-	✓	-	-	-
1990	1370	MAC-005-1126	S	Pelagic	✓	-	✓	-	-	-
1997	1607	MAC-200	S	Pelagic	-	-	✓	-	✓	2.9
1998	1611	END-130	N	Pelagic	✓	-	-	-	✓	2.1
1999	1614	MAC-068	S	Pelagic	✓	-	✓	-	✓	1.6
2000	1616	MAC-052	S	Pelagic	-	-	✓	-	-	-
2002	1621	DSJ-184	S	Pelagic	-	-	✓	✓	✓	2.8
2005	1629	MII-061	N	MHI	✓	-	-	-	-	-
2005	1629	MII-151	S	Pelagic	✓	-	✓	-	✓	1.8
2005	1629	MII-155	S	Pelagic	✓	-	✓	-	✓	1.3
2005	1629	MII-200	S	Pelagic	✓	-	✓	-	✓	1.2
2005	1629	MII-204	S	Pelagic	✓	-	✓	-	✓	2.1
2005	1629	MII-207	S	Pelagic	-	-	✓	-	✓	0.9
2005	1629	MII-216	S	Pelagic	✓	-	✓	-	✓	1.8
2005	1629	MII-219	S	Pelagic	✓	-	✓	-	✓	2.4
2006	1631	MII-041	S	Pelagic	✓	-	✓	-	-	-

Year	Survey No.	Sighting No.[1]	Effort	Population	$f(0)$	$E(s)$	$g(0)^2$	n/L – Design	n/L – Model	n Pelagic
2006	1631	MII-056	S	Pelagic	✓	-	✓	-	-	-
2006	1631	MII-120	S	Pelagic	-	-	✓	-	✓	1.3
2006	1631	MII-128	S	Pelagic	✓	-	✓	-	✓	3.4
2006	1631	MII-141	S	Pelagic	✓	-	✓	-	-	-
2009	0901	OES-049	S	MHI or pelagic	✓	-	✓	-	✓	0.2
2009	0901	OES-071	S	MHI	✓	-	✓	-	-	-
2009	0901	OES-079	S	MHI or pelagic	✓	-	✓	-	✓	0.2
2009	0901	OES-082	S	MHI	✓	-	✓	-	-	-
2010	1004	OES-005	S	Pelagic	✓	-	-	-	-	-
2010	1641	MII-035	S	Pelagic	✓	-	✓	✓	✓	3.1
2010	1641	MII-098	S	Pelagic	✓	-	✓	✓	✓	1.0
2010	1641	MII-103	S	Pelagic	✓	-	✓	✓	✓	1.0
2010	1641	MII-140	N	NWHI	✓	-	-	-	-	-
2010	1641	MII-142	N	NWHI	✓	-	-	-	-	-
2010	1641	MII-224	N	MHI	✓	-	-	-	-	-
2010	1641	MII-231	S	Pelagic	✓	-	✓	✓	✓	1.0
2010	1641	MII-241	S	Pelagic	✓	-	✓	✓	✓	6.4
2010	1642	OES-086	S	NWHI	✓	-	✓	✓	-	-
2011	1108	OES-004	S	Pelagic	✓	✓	✓	-	✓	4.0
2012	1203	OES-037	O	Pelagic	-	✓	-	-	-	-
2012	1203	OES-068	O	Pelagic	-	✓	-	-	-	-
2012	1203	OES-069	N	Pelagic	-	-	-	-	✓	1.0
2012	1203	OES-071	O	Pelagic	-	✓	-	-	-	-
2013	1303	OES-013	S	NWHI or pelagic	✓	✓	✓	-	✓	1.2
2013	1303	OES-020	O	Pelagic	-	✓	-	-	-	-
2013	1303	OES-059	S	Pelagic	✓	✓	✓	-	✓	1.5
2013	1303	OES-062	S	NWHI or pelagic	✓	✓	✓	-	✓	2.4
2013	1303	OES-089	O	NWHI or pelagic	-	✓	-	-	-	-
2016	1604	OES-018	S	MHI	✓	-	✓	-	-	-
2016	1604	OES-021	O	MHI or pelagic	-	✓	-	-	-	-
2016	1604	OES-026	O	MHI or NWHI or pelagic	-	✓	-	-	-	-

Year	Survey No.	Sighting No.[1]	Effort	Population	$f(0)$	$E(s)$	$g(0)$[2]	n/L – Design	n/L – Model	n Pelagic
2017	1705	LAS-016	O	Pelagic	-	✓	-	-		-
2017	1705	LAS-055	N	MHI or pelagic	✓	✓	-	-	✓	0.2
2017	1705	LAS-056	N	MHI or pelagic	✓	✓	-	-	✓	0.8
2017	1705	LAS-064	S	Pelagic	✓	✓	✓	✓	✓	2.0
2017	1705	LAS-073	S	Pelagic	✓	✓	✓	✓	✓	6.0
2017	1705	LAS-086	O	MHI	-	✓	-	-	-	-
2017	1705	LAS-114	O	NWHI or pelagic	-	✓	-	-	-	-
2017	1705	LAS-115	O	Pelagic	-	✓	-	-	-	-
2017	1705	LAS-116	O	Pelagic	-	✓	-	-	-	-
2017	1705	LAS-125	N	NWHI or pelagic	✓	✓	-	-	✓	3.6
2017	1705	LAS-136	O	MHI	-	✓	-	-	-	-
2017	1705	LAS-159	N	Pelagic	✓	-	-	-	✓	1.0
2017	1706	OES-001	N	MHI or pelagic	✓	✓	-	-	✓	0.6
2017	1706	OES-020	O	MHI or pelagic	-	✓	-	-	-	-
2017	1706	OES-033	S	Pelagic	✓	✓	✓	✓	✓	4.0
2017	1706	OES-039	S	Pelagic	✓	✓	✓	✓	✓	4.0
2017	1706	OES-116	O	MHI or pelagic	-	✓	-	-	-	-
2017	1706	OES-119	N	Pelagic	✓	✓	-	-	✓	11.0
2017	1706	OES-122	S	Pelagic	✓	✓	✓	✓	✓	3.0
2017	1706	OES-133	S	NWHI or pelagic	✓	✓	✓	✓	✓	3.6
2017	1706	OES-141	S	Pelagic	✓	✓	✓	✓	✓	1.0
2017	1706	OES-176	S	MHI	✓	✓	✓	-	-	-

Sightings were made during systematic (S) or nonsystematic (N) effort or while off-effort (O) and were assigned when possible to either the main Hawaiian Island (MHI), Northwestern Hawaiian Islands (NWHI), or pelagic population. The use of each sighting is denoted by a checkmark in one or more parameter columns: $f(0)$ is the probability density function of the perpendicular detection distances evaluated at zero distance used in the design-based approach; $E(s)$ is the expected size of false killer whale subgroups; $g(0)$ is the probability of detection on the trackline; and n/L is the encounter rate for either the design- or model-based approach. The number of subgroups (n) applicable to the encounter rates of each approach is shown for the pelagic population.

[1]Sighting numbers were reset at 001 each day during the 1986−1990 surveys, so the month and day (mmdd) of each sighting was added to provide a unique identifier for sightings from those years.

[2]The $g(0)$ estimation used 62 additional sightings from the eastern tropical Pacific that are not listed here.

Appendix B: Evaluation of Higher-density Survey Effort in 2017

During the Hawaiian Islands Cetacean and Ecosystem Assessment Survey (HICEAS) of 2017, "fine-scale" survey effort was recorded when visual observers were on-effort within the main Hawaiian Islands (MHI) stratum while the ship was transiting to and from the systematic parallel transect lines for the purposes of deploying or recovering drifting acoustic spar buoy recorders (DASBRs). The random selection of DASBR deployment locations and the subsequent, seemingly random movement of DASBRs prior to their retrieval appeared to provide an opportunity for additional systematic survey effort within this stratum. Visual inspection of the fine-scale survey effort suggested it may not have provided representative sampling of the MHI stratum, so an analysis was undertaken to determine whether this effort should be included as systematic effort when estimating encounter rates for the design-based approach.

The 10 km effort segments and the ~9 km × 9 km grid from the species distribution model (SDM) were used to evaluate whether the fine-scale effort was representative of the overall MHI stratum study area. Specifically, the midpoints of the effort segments and the 2,855 grid cell midpoints within the MHI stratum were compared relative to two static variables: depth and distance to land. A two-sample Kolmogorov-Smirnoff (K-S) test was used to compare the distribution of each variable from the effort segments to that from the stratum. Three effort combinations were evaluated: fine-scale effort alone, parallel transect effort alone, and the combination of fine-scale and parallel transect effort (Figure B 1).

In general, the MHI stratum consists of deep water, with most grid cells having water depths between 4000 m and 5000 m (Figure B 2A). The distribution of water depths between 0 m and 4000 m is relatively uniform, with a slight dip from 1000 m to 2000 m. The MHI stratum encompasses nearshore waters of the MHI by design, so the grid cells are strongly biased toward distances to land under 100 km, with a relatively uniform distribution of distances between 0 km and 100 km (Figure B 2B). In contrast, the fine-scale effort was conducted in water depths with a nearly uniform distribution from 500 m to 5000 m (Figure B 2C) and primarily within 40 km of land (Figure B 2D). The distribution of parallel transect effort more closely matches the underlying depth and distance-to-land distribution of the MHI stratum, although with relatively less effort in the waters <500 m and within 20 km of land (Figure B 2E−F). The qualitative comparison of the distributions of depth and distance to land between each type of survey effort and the MHI stratum is supported by the K-S tests, which found a significant difference (i.e., *p*-value <0.05) between the fine-scale effort and the MHI stratum for both variables and no significant difference between the parallel transect effort and the MHI stratum for both variables (Table B 1).

These results indicate that the fine-scale survey effort oversampled shallow waters closer to land and is not representative of the MHI stratum based on these static variables. However, the combination of the fine-scale effort and the representative parallel transect effort may have ultimately provided representative coverage of the MHI stratum. The depth and distance to land distributions of the combined effort types do more closely approach the distributions of those variables within the MHI stratum. However, there is greater representation of intermediate depths (i.e., 500 m to 4000 m; Figure B 2G) and smaller distances to land, particularly within 20−40 km of land (Figure B 2H) relative to the MHI stratum distributions. The results of the K-S

tests indicate that the combination of fine-scale and parallel transect effort does not ultimately provide a representative sample of the depth and distance to land within the MHI stratum (Table B 1). Overall, this evaluation determined the fine-scale effort could not be used without biasing the survey effort in the MHI stratum to shallower waters closer to land. Therefore, the fine-scale effort was considered to be nonsystematic and was not included in the encounter rate analysis for the design-based approach. The effort was still used when developing the encounter rate model of the SDM, as there is no similar requirement for randomized effort within that framework.

Table B 1. Results of the Kolmogorov-Smirnoff (K-S) tests comparing the distribution of depth and distance to land from the main Hawaiian Islands stratum to those from areas sampled by fine-scale and parallel transect effort within the stratum, including the corresponding midpoint sample size (n). *D* is the K-S test statistic. Significant results (*p*-value < 0.05) are shown in bold.

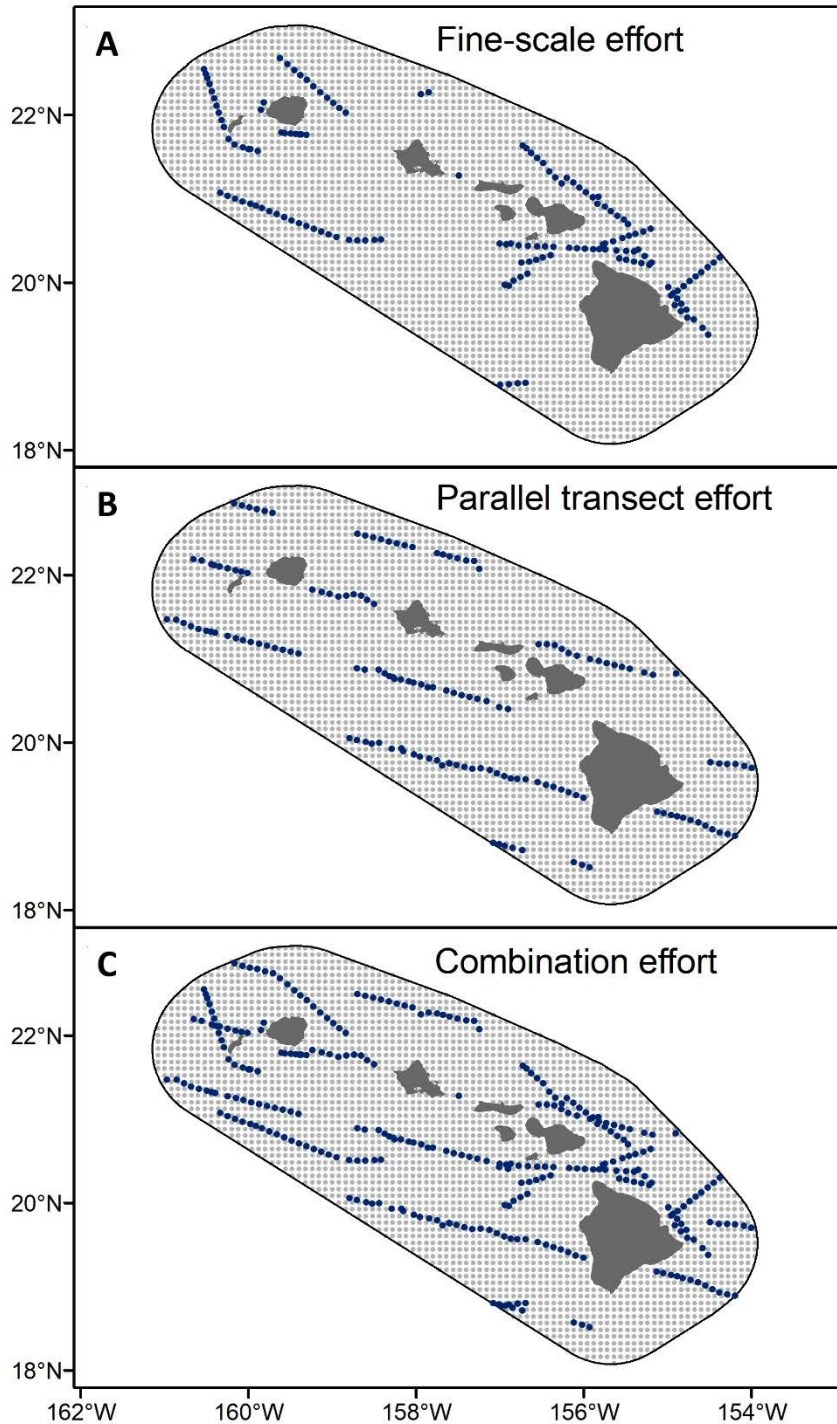| Effort Type	n	Depth *D*	*p*-value	Distance to Land *D*	*p*-value
Fine-scale	148	0.292	**<0.001**	0.285	**<0.001**
Parallel transect	151	0.099	0.118	0.103	0.095
Fine-scale and parallel transect	299	0.108	**0.004**	0.117	**0.001**

Figure B 1. Maps of the survey effort midpoints (blue circles) and ~9km × 9km grid points (light gray circles) that were compared to evaluate whether the fine-scale effort was representative of the overall main Hawaiian Island (MHI) stratum (outlined in black), where effort evaluated was either (A) fine-scale effort, (B) parallel transect effort, or (C) the combination of fine-scale and parallel transect effort.
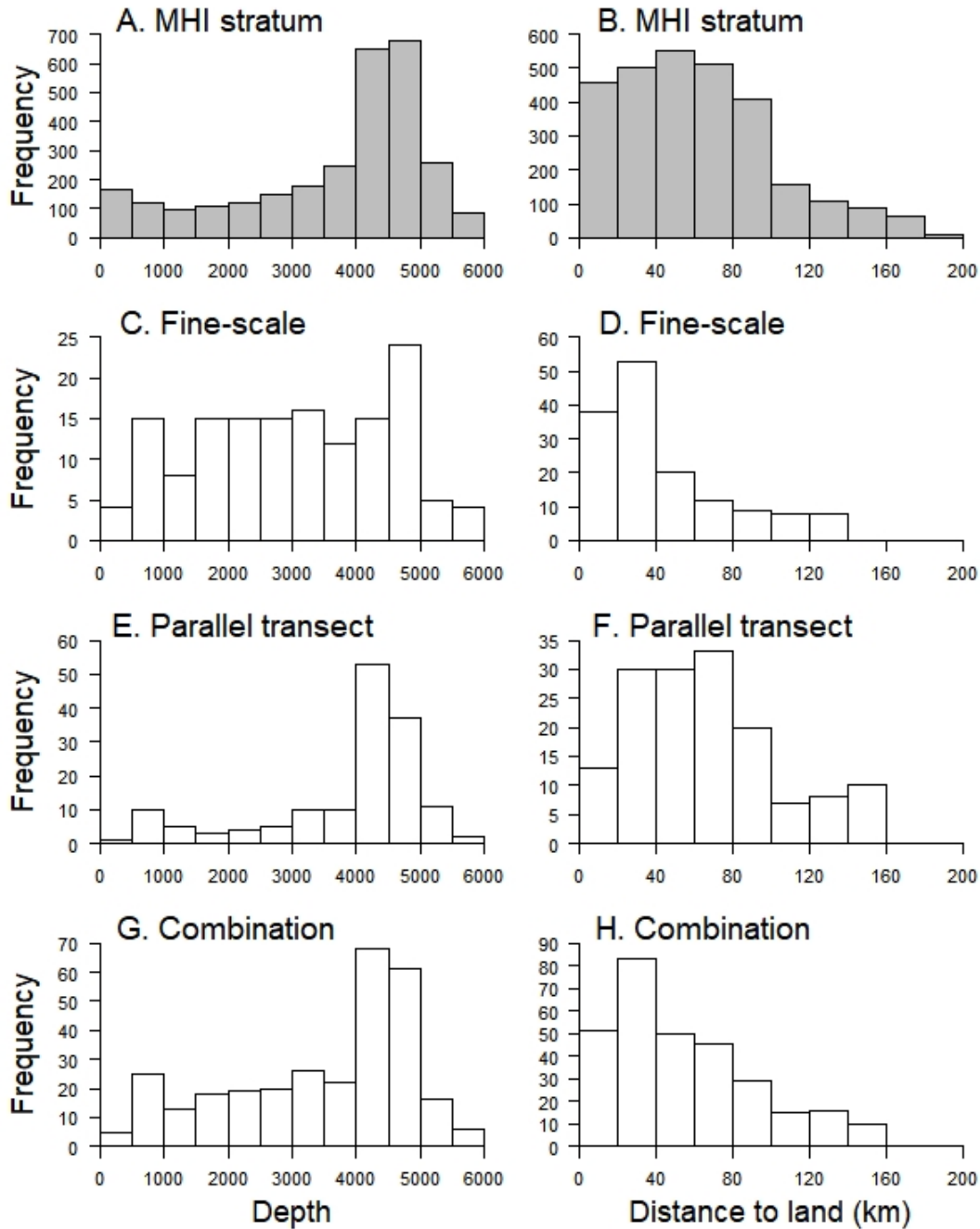
The MHI are shown in gray.

Figure B 2. Distribution of depth and distance to land throughout the main Hawaiian Island (MHI) stratum and for each of the effort types evaluated, where (A) and (B) show the underlying distribution of depth and distance to land, respectively, for the entire MHI stratum (gray bars), and (C) and (D), (E) and (F), and (G) and (H) show the distribution of these variables during fine-scale effort, parallel transect effort, and the combination of fine-scale and parallel transect effort, respectively (white bars).

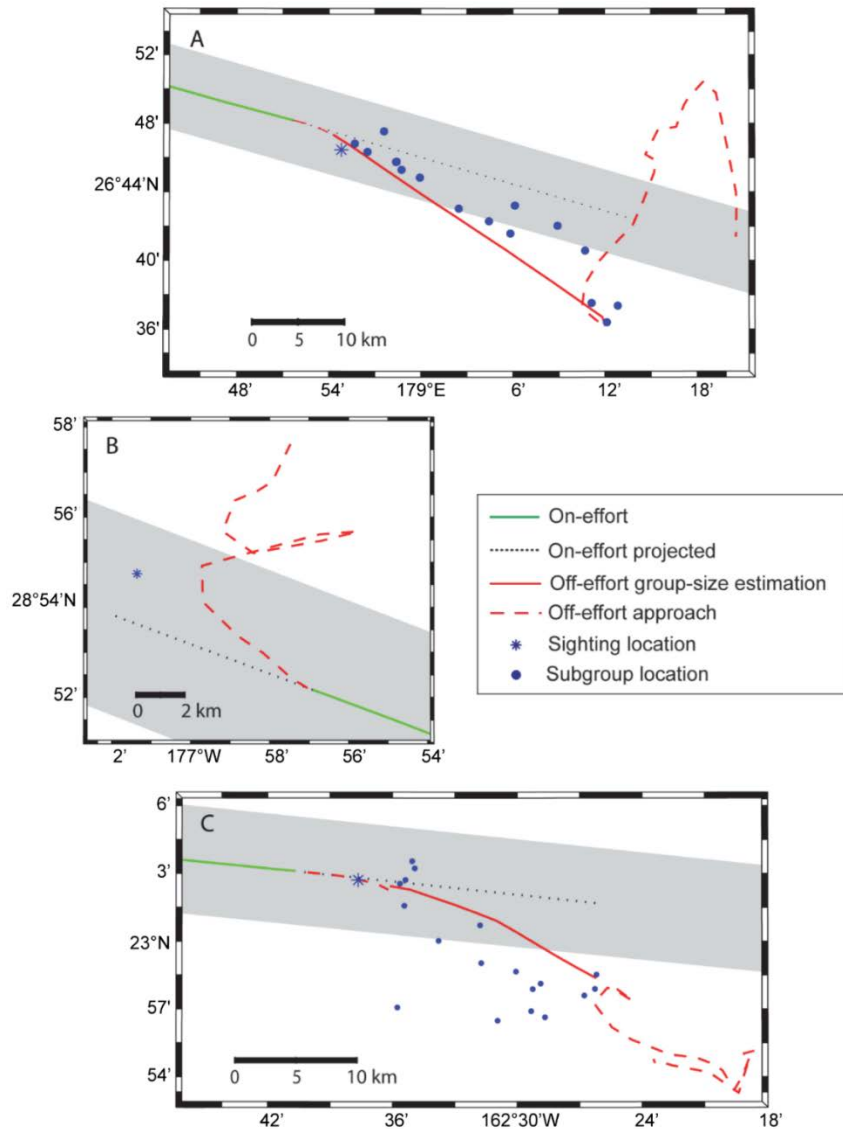# Appendix C: False Killer Whale Sighting Schematics

Figure C 1. Schematics of the systematic-effort false killer whale sightings for which the group-size estimation protocol was attempted during the Hawaiian Islands Cetaceans and Ecosystem Assessment Survey of 2010, with (A) sighting MII-241 and (B) sighting MII-035 of the pelagic population, and (C) sighting OES-086 of the Northwestern Hawaiian Islands population.

"On-effort projected" is the track the ship would have taken if systematic-effort status had been maintained. "Off-effort group-size estimation" represents the implementation of the group-size estimation protocol, with the localized subgroups shown as blue circles (except during MII-035 when subgroups could not be localized). "Off-effort approach" is the track associated with approaching the group for photo-identification and biopsy sampling. The sighting location refers to the initial visual detection that prompted the group-size estimation protocol. The gray shading denotes the 4.5-km analytical truncation distance. Figure reprinted from Bradford et al. (2014).
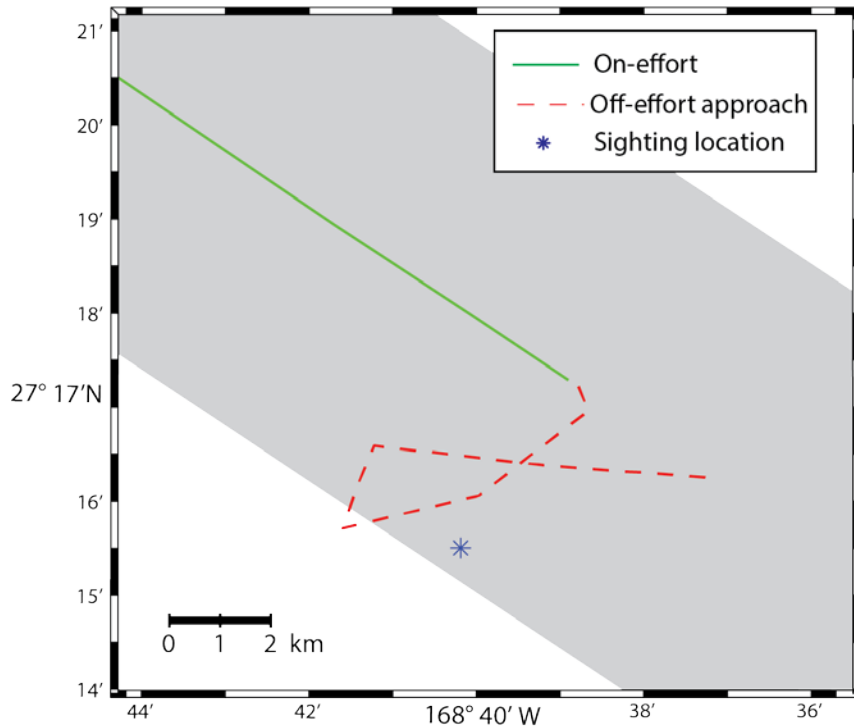
Figure C 2. Schematic of the systematic-effort sighting DSJ-184 of the pelagic false killer whale population made during the Hawaiian Islands Cetacean and Ecosystem Assessment Survey of 2002.

"Off-effort approach" is the track associated with approaching the group for photo-identification and biopsy sampling. The sighting location refers to the initial visual detection that prompted the close on the group. The gray shading denotes the 4.5-km analytical truncation distance.

Appendix D: Revised Stock Boundary for Hawaiʻi Pelagic False Killer Whales

The stock boundaries for the three populations of false killer whales in Hawaiian waters were revised in 2015 (Bradford et al. 2015). Most of the data that informed the boundary revisions were satellite telemetry data (n = 6 tracks from 2008 to 2014) collected by the Cascadia Research Collective (CRC; n = 4 tracks) and the Pacific Islands Fisheries Science Center (PIFSC; n = 2 tracks). The goals of the revision process were to produce stock boundaries that reflect uncertainty and are robust to routine inputs from ongoing data collection. A specific objective for the pelagic false killer whale population was for the inner stock boundary to include the full extent of the observed range.

Prior to the 2015 revision, available sighting and telemetry data suggested pelagic false killer whales did not occur within 40 km of the main Hawaiian Islands (MHI). However, data collected by CRC during 2013−2014 indicated that pelagic false killer whales do occur closer to land within the MHI (Bradford et al. 2015). Consequently, the inner stock boundary for the pelagic population was reduced from a 40-km to an 11-km radius around the MHI based on the telemetry location nearest to land (Figure D 1A). However, the rarity of pelagic false killer whale sightings and known movements within nearshore waters (less than 2,000 m in depth and within 100 km of shore) around the MHI was documented.

Since the 2015 revision, three pelagic false killer whales were satellite-tagged by PIFSC off Kauai in the MHI during the Hawaiian Islands Cetacean and Ecosystem Assessment Survey (HICEAS) of 2017 (Yano et al. 2018). While tagged in two separate sightings on consecutive days in mid-September, the three individuals were part of the same group and traveled together during the period the satellite tags were simultaneously active, although the tag durations varied (4, 22, and 179 days, respectively). After filtering the received locations from these tags using the Douglas Argos Filter (Douglas et al. 2012) following Baird et al. (2010; 2012) and then examining only locations of known accuracy, the closest distance to land of a received location in the MHI was 5.9 km (with an estimated error radius of 705 m; Table D 1). Of the 345 locations in the vicinity of the MHI, 10 (2.9%) were within 11 km of land (Table D 1; Figure D 2). While few in number, these movements close to the MHI occurred over 28 days during September and October, a period when the whales generally remained in nearshore waters of the MHI (127 of 163, or 77.9%, of locations within 100 km of land).

The new satellite telemetry data indicate that pelagic false killer whales do occur within 11 km of land in the MHI and that the current inner stock boundary is no longer valid (Figures D 1B and 2). Further, the few but repeated movements inside the established inner stock boundary suggest that eliminating that boundary altogether is most consistent with the stated goals and objectives of false killer whale stock boundary revisions (Bradford et al. 2015).

The new data also show that the frequency with which pelagic false killer whales use nearshore waters of the MHI is somewhat greater than previously considered. The assessment of the telemetry data in Bradford et al. (2015) revealed that pelagic false killer whales may select more strongly for depth than distance to land and use the nearshore waters of the MHI and Northwestern Hawaiian Islands (NWHI) differently. Specifically, the nearshore use of pelagic false killer whales tagged off Hawaiʻi Island in the MHI was compared to that of pelagic false

killer whales tagged in the NWHI. This comparison found that only 0.3% of locations within the MHI occurred at water depths less than 2,000 m, while 8.2% of the locations in the NWHI occurred within that bathymetric contour.

This comparison was repeated with the current set of available satellite telemetry data using only locations of known accuracy (n = 1,523) from independent tracks (n = 5). The individual represented by the independent track from HICEAS 2017 spent time in both the MHI and NWHI (Figure D 1B). Thus, locations from all tracks were grouped by their proximity to either the MHI or NWHI instead of by where the individuals were tagged. The easternmost point of the Papahānaumokuākea Marine National Monument (PMNM) was used as a demarcation between the MHI and NWHI (Figure D 3). Pelagic false killer whales were again found to use nearshore waters less frequently around the MHI than the NWHI, with 31 (5.0%) of the 616 MHI locations within 2,000 m depth (Figure D 4A-B) versus 68 (7.5%) of the 907 NWHI locations (Figure D 4C−D), though the relative difference in use of shallower waters was much lass marked than the 2015 comparison.

Although it is appropriate to remove the inner stock boundary to reflect the nearshore use of the MHI by pelagic false killer whales, this population is still rare within this region. CRC has conducted small-boat surveys for odontocete cetaceans around the MHI 1−6 times per year since 2000. From 2000 through 2019, false killer whales have been sighted 76 times within 100 km from shore during these surveys. Of these sightings, only 3 (3.9%) are known to be of the pelagic population, with 67 of the remaining sightings being of the MHI insular population, 4 of the NWHI population, and 2 of unknown population identity (R. Baird, unpublished data). Current stock boundaries for cetaceans in Hawaiian waters largely represent the full range of each population within the U.S. Hawaiian Islands Exclusive Economic Zone. If future stock boundary revisions incorporate additional information to develop probabilistic surfaces representing likelihood of occurrence, a reduced likelihood of occurrence in nearshore waters of the MHI may be considered.

Table D 1. Information associated with the locations of two satellite-tagged pelagic false killer whales that came within 11 km of the main Hawaiian Islands.

Tag ID	Date	Time	Location Class	Error Radius	Distance to Land	Depth
141703	**09/21/2017**	**05:13:36**	**L2**	**349**	**6.4**	**1,062**
141702	**09/21/2017**	**05:13:59**	**L2**	**324**	**10.6**	**1,347**
141703	**09/21/2017**	**06:24:34**	**L1**	**705**	**5.9**	**587**
141703	**09/21/2017**	**07:04:04**	**L3**	**180**	**10.5**	**1,347**
141702	**10/11/2017**	**05:15:26**	**L3**	**233**	**6.3**	**1,304**
141702	10/13/2017	05:11:57	L2	483	9.6	2,080
141702	10/13/2017	05:25:03	L2	277	10.0	2,233
141702	10/15/2017	17:33:29	L2	280	9.8	1,355
141702	10/18/2017	06:07:14	L1	863	10.7	1,805
141702	**10/18/2017**	**18:05:22**	**L1**	**588**	**8.7**	**1,206**

The date and time are in Greenwich Mean Time, the location class and error radius (in m) were provided by the Argos satellite system, and the distance to land and depth are shown in km and m, respectively. Rows highlighted in bold correspond to the 6 locations within the inner stock boundary in Figure D 2.
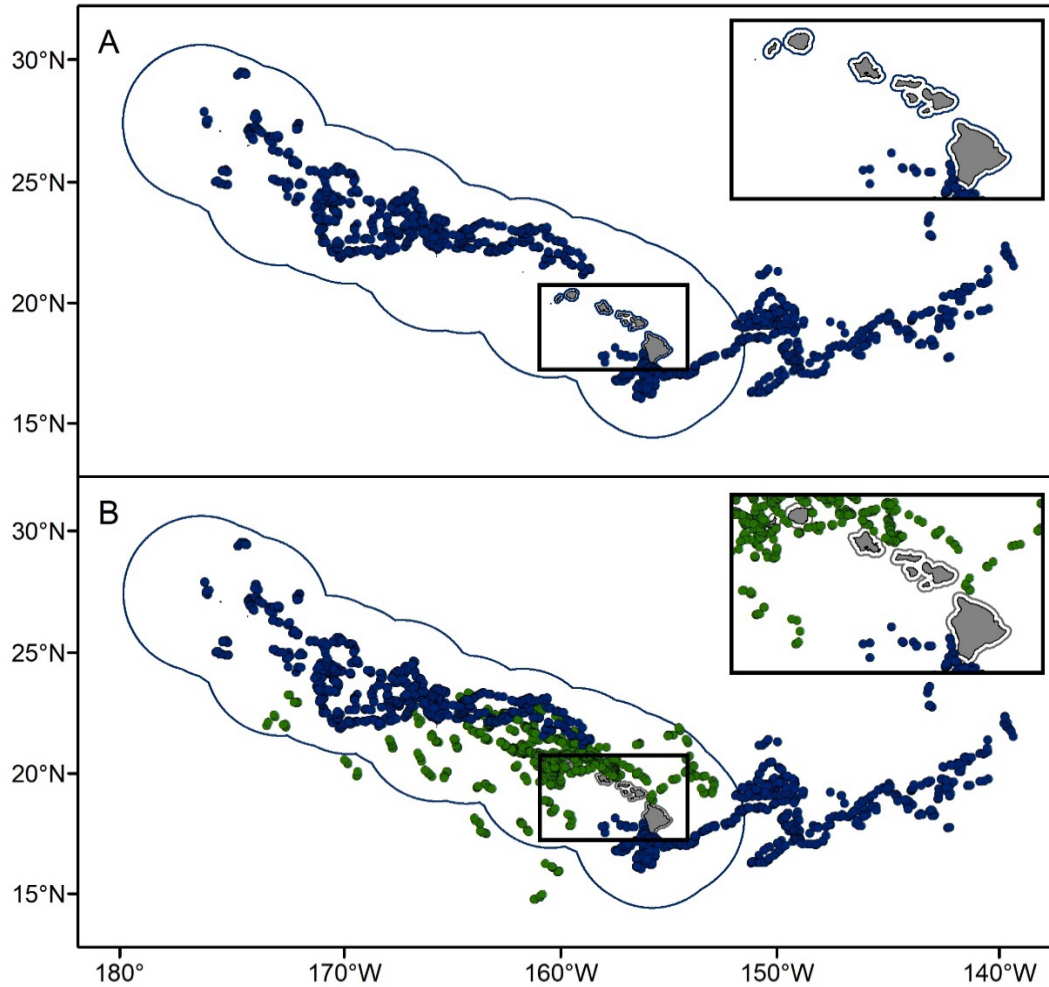
Figure D 1. Pelagic false killer whale satellite telemetry locations available for the Bradford et al. (2015) stock boundary revision (blue circles; n = 2,125) and those added for the current revision (green circles; n = 1,060), with (A) showing the inner stock boundary (blue line in inset of main Hawaiian Islands) established in 2015, and (B) showing elimination of the inner stock boundary (gray line) given the nearshore movements reflected in the recent data.

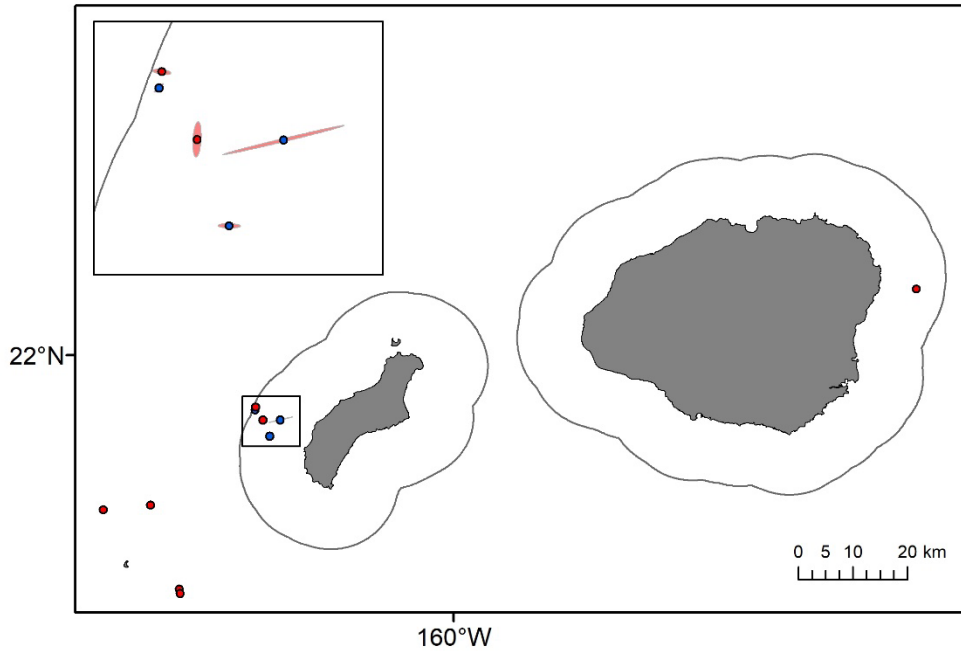The outer blue outline is the U.S. Hawaiian Islands Exclusive Economic Zone.

Figure D 2. Locations of two satellite-tagged pelagic false killer whales (red and blue circles; n = 10) that came within 11 km of the main Hawaiian Islands.

Four of these locations were in proximity of Kaʻula Rock (lower left corner), which was not encompassed in the inner stock boundary (gray line). The remaining six locations were within the inner stock boundary, with the inset showing the five locations in proximity of Niʻihau. The red polygons around each point are the Argos error ellipses.
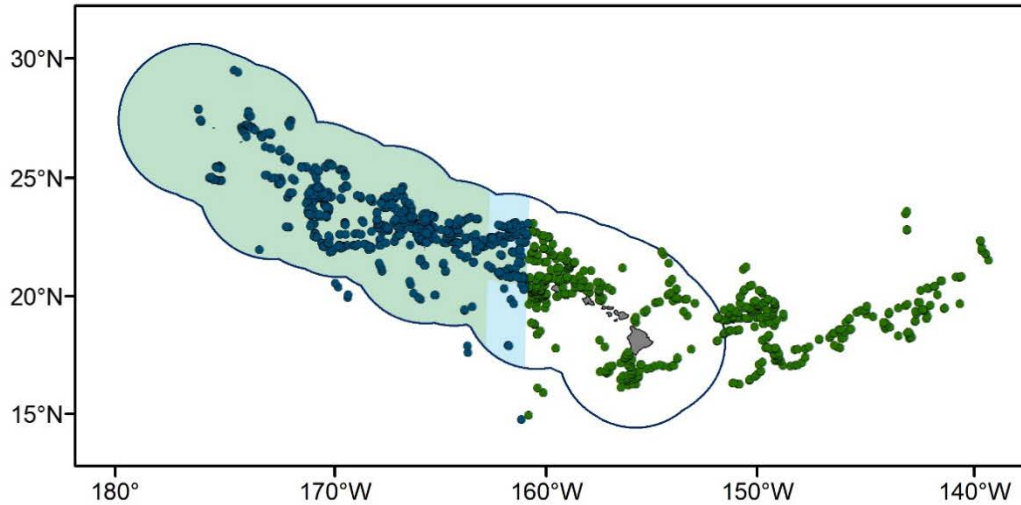
Figure D 3. Locations of known accuracy (n = 1,523) from independent satellite telemetry tracks (n = 5) used to evaluate differences in nearshore use by pelagic false killer whales in the main Hawaiian Islands (MHI) (green circles; n = 616) and the Northwestern Hawaiian Islands (NWHI) (blue circles; n = 907).

The area shaded in light green is the Papahānaumokuākea Marine National Monument (PMNM). The area shaded in light blue shows how the eastern edge of the PMNM was extended for the purposes of assigning locations to the proximity of the NWHI or MHI. The outer blue line is the U.S. Hawaiian Islands Exclusive Economic Zone.
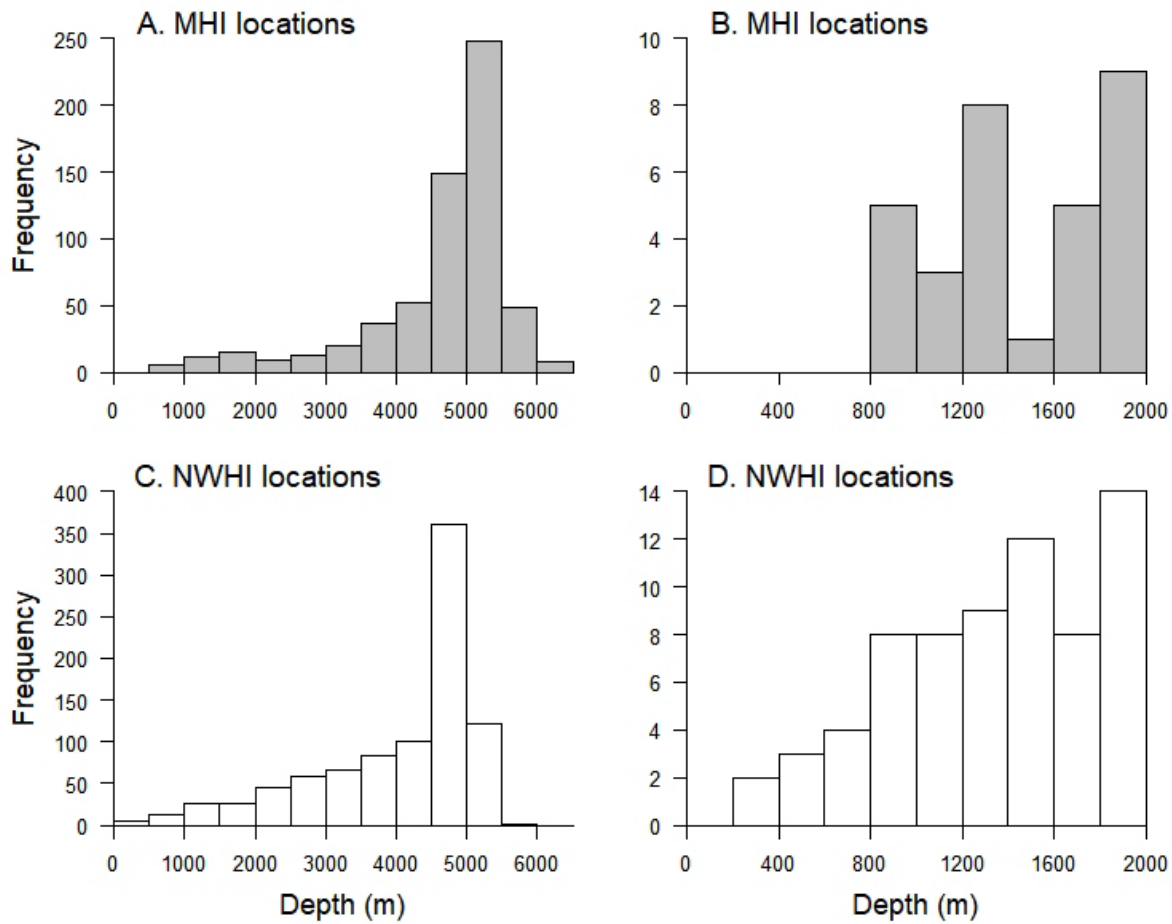
Figure D 4. Distribution of depth used by pelagic false killer whales in the proximity of the main Hawaiian Islands (MHI; gray bars), showing (A) all locations (n = 616) and (B) locations in waters less than 2,000 m (n = 31), and of the Northwestern Hawaiian Islands (NWHI; white bars), showing (C) all locations (n = 907) and (D) locations in waters less than 2,000 m (n = 68).

Histograms are based on independent satellite tracks and locations of known accuracy.

Appendix E: Model-predicted Encounter Rates of Pelagic False Killer Whales
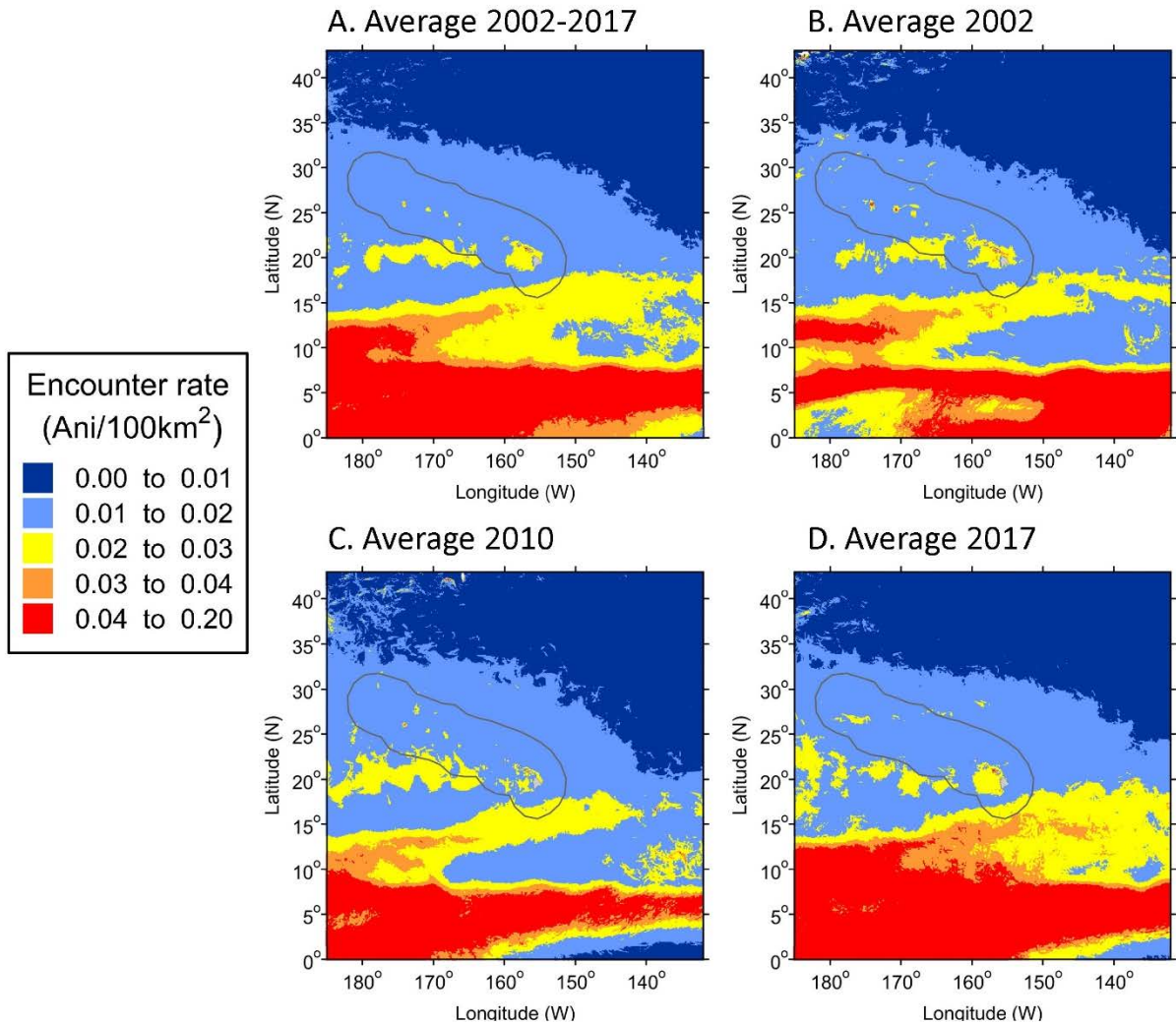

Figure E 1. Predicted encounter rates (without the influence of the group size model) for pelagic false killer whales in the central Pacific study area based on tri-daily predictions averaged across (A) all years (2002, 2010, and 2017), (B) 2002, (C) 2010, and (D) 2017 (see text for details).

The range of values shown for the encounter rate are defined by linear increments specific to the average and used in the yearly maps for comparison.

Appendix F: Proportions of Systematic Survey Effort by Beaufort Sea State

Table F 1. Proportions of systematic survey effort in Beaufort sea states 0 to 6 by survey year and stratum used in the design-based approach to compute a weighted average of the Beaufort-specific probabilities of detection on the trackline for the Northwestern Hawaiian Islands (NWHI) and pelagic populations of false killer whales in the U.S. Exclusive Economic Zone (EEZ) of the Hawaiian Islands.

Beaufort	2010 NWHI – EEZ	2017 NWHI – EEZ	2002 pelagic – outer EEZ	2010 pelagic – EEZ	2017 pelagic – EEZ
0	0.001	0.004	0.008	0.001	0.001
1	0.010	0.022	0.015	0.012	0.009
2	0.113	0.077	0.045	0.041	0.043
3	0.159	0.137	0.100	0.124	0.122
4	0.425	0.291	0.491	0.474	0.316
5	0.283	0.303	0.311	0.301	0.344
6	0.009	0.166	0.030	0.046	0.165

Appendix G: Summary and Diagnostics of Encounter Rate and Group Size Models

```
Where 'spline2use' = "ts" and 'maxdf' = 10

Family: Tweedie(p=1.01)
Link function: log

Formula:
er ~ offset(log(effort)) + s(SST, bs = spline2use, k = maxdf) +
    s(SSTsd, bs = spline2use, k = maxdf) + te(SSH, mlat, bs = spline2use, k = 5)

Parametric coefficients:
            Estimate Std. Error t value Pr(>|t|)
(Intercept)  -8.8152     0.1908   -46.2   <2e-16 ***
---
Signif. codes:  0 '***' 0.001 '**' 0.01 '*' 0.05 '.' 0.1 ' ' 1

Approximate significance of smooth terms:
               edf Ref.df      F p-value
s(SST)        0.8388      9 0.474 0.01627 *
s(SSTsd)      0.8314      9 0.649 0.00762 **
te(SSH,mlat)  2.9119     24 0.378 0.00877 **
---
Signif. codes:  0 '***' 0.001 '**' 0.01 '*' 0.05 '.' 0.1 ' ' 1

R-sq.(adj) =  0.00237   Deviance explained = 4.37%
-REML = 201.18  Scale est. = 1.0677     n = 11593
```

Figure G 1. Summary call of the encounter rate generalized additive model used in the model-based approach from the package 'mgcv' (Wood 2011) in R (R Core Team 2017).

```
Where 'spline2use' = "ts" and 'maxdf' = 10

Family: gaussian
Link function: identity

Formula:
log(avegs) ~ +s(MLD, bs = spline2use, k = maxdf)

Parametric coefficients:
            Estimate Std. Error t value Pr(>|t|)
(Intercept)    1.377      0.138   9.977 6.33e-12 ***
---
Signif. codes:  0 '***' 0.001 '**' 0.01 '*' 0.05 '.' 0.1 ' ' 1

Approximate significance of smooth terms:
          edf Ref.df     F p-value
s(MLD) 0.8566      9 0.512  0.0243 *
---
Signif. codes:  0 '***' 0.001 '**' 0.01 '*' 0.05 '.' 0.1 ' ' 1

R-sq.(adj) =  0.111   Deviance explained = 13.1%
-REML = 49.226  Scale est. = 0.72332   n = 38
```
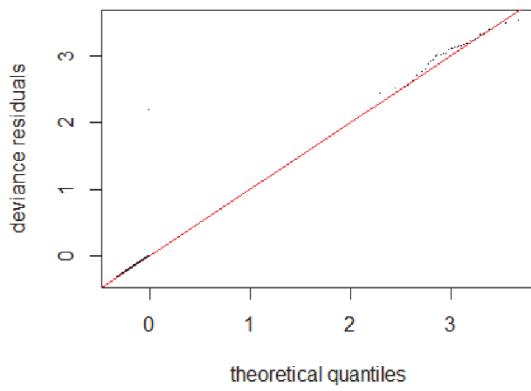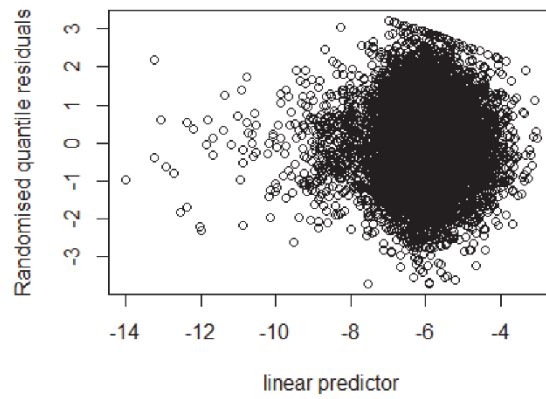
Figure G 2. Summary call of habitat-based group size generalized additive model used in the model-based approach from the package 'mgcv' (Wood 2011) in R (R Core Team 2017).

Encounter rate model diagnostics

Q-Q plot

Residuals vs. linear predictor plot

Group size model diagnostics
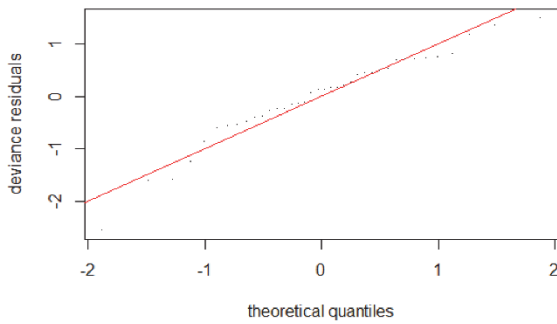
Q-Q plot

Figure G 3. Diagnostic plots of the habitat-based encounter rate and group size generalized additive models used in the model-based approach from the package 'mgcv' (Wood 2011) in R (R Core Team 2017).

Appendix H: The Role of Random Variation in the Design-based Encounter Rate

A simulation study was conducted to evaluate whether the low and high encounter rate of pelagic false killer whales during the Hawaiian Islands Cetacean Ecosystem and Assessment Survey (HICEAS) of 2002 and 2017, respectively, could have occurred by chance if the overall abundance of the population within the U.S. Hawaiian Islands Exclusive Economic Zone (Hawaiian EEZ) did not change during the study period. Consistent with the encounter rate variance estimation in the design-based approach, 150-km segments of systematic survey effort were created for each HICEAS year (2002, 2010, and 2017). These effort segments were linked to their associated number of sightings and subgroups (actual or expected; Tables 2 and H1) and then pooled for use in a bootstrap procedure. Because systematic survey effort was stratified between the main Hawaiian Islands (MHI) and the outer EEZ in 2002, with a higher density of effort in the MHI stratum, effort segments from each year were classified by stratum to make the bootstrap procedure compatible over all years. Effort segments were sampled with replacement 1000 times according to the number of segments surveyed in each stratum in each year (i.e., fewer effort segments were drawn in the MHI stratum in 2010 and 2017 than in 2002; Table H 1). For each bootstrap iteration, the number of false killer whale sightings and the number of subgroups were each summed over all effort segments in the sample.

The distribution of the simulated number of sightings and subgroups for each HICEAS year is shown in Figure H 1. Because of the potential biases associated with the expected number of subgroups in 2002 and 2010, the number of sightings is likely a better measure of the variability in encounter rates across all HICEAS years. The simulated number of sightings in each survey year has a peak between three and five sightings, although the shape of the distribution varies slightly among years. The simulated number of sightings in 2010 was close to what was observed, with 17.9% of iterations containing 5 sightings (the observed number of sightings in that year) and 48.8% of them containing 4−6 sightings. However, the simulated number of sightings in 2002 and 2017 was somewhat higher and lower, respectively, than what was observed, with 6.6% of iterations containing ≤1 sighting in 2002, and 12.6% of iterations containing ≥7 sightings in 2017. While these simulated probabilities are relatively small, they indicate the observed encounter rates could have occurred by chance when abundance was constant. Thus, random variation in encounter rate may be playing a pronounced role in the design-based density estimates. However, the fact that these probabilities are relatively low does not exclude the possibility that other factors are also influencing the resulting estimates, including changes in false killer whale abundance within the Hawaiian EEZ as a result of shifts in distribution within the broader central Pacific.

Table H 1. Number of systematic survey effort segments and total survey distance (km) in each survey stratum in each year of the Hawaiian Islands Cetacean and Ecosystem Assessment Survey (HICEAS), where stratum is in either the main Hawaiian Islands (MHI) or outer U.S. Exclusive Economic Zone (EEZ) of the Hawaiian Islands.

Year	MHI segments	MHI distance	Outer-EEZ segments	Outer-EEZ distance	Sightings	Subgroups
2002	30	3,540	99	13,473	1	2.8
2010	15	1,739	106	14,405	5	12.5
2017	14	1,352	111	14,858	7	23.6

The number of pelagic false killer whale sightings and associated subgroups (actual or expected) observed during each HICEAS year was compared to the simulated distributions in Figure H 1.
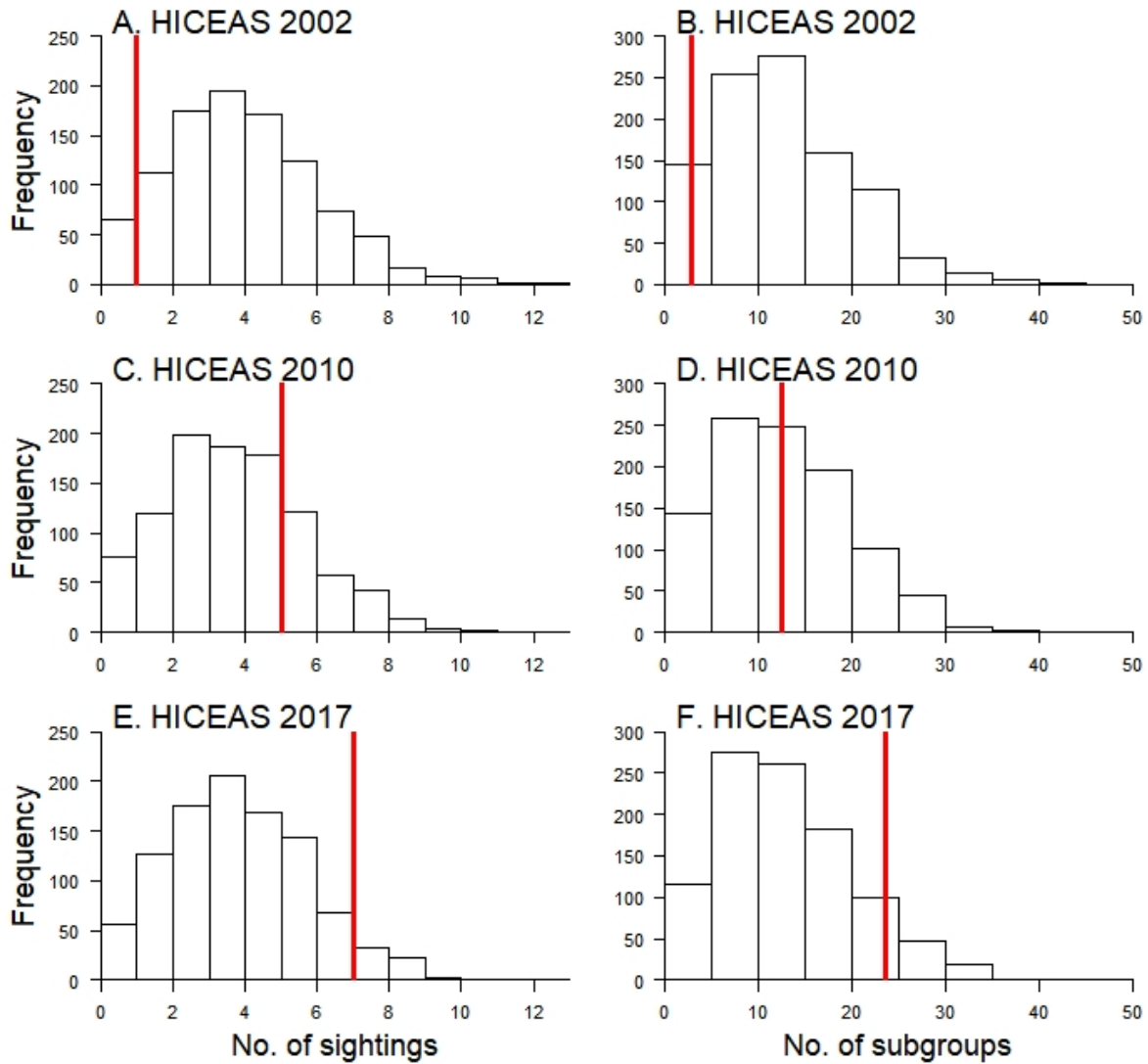
Figure H 1. Distributions of the simulated number of pelagic false killer whale sightings and subgroups resulting from the bootstrap for each year of the Hawaiian Islands Assessment and Ecosystem Assessment Survey (HICEAS), where (A) and (B) are the distributions of sightings and subgroups, respectively, for HICEAS 2002, (C) and (D) are the distributions for HICEAS 2010, and (E) and (F) are the distributions for HICEAS 2017.

The number of sightings and associated subgroups (actual or expected) actually observed during each HICEAS year is represented by the red line.